



Tartu University

Faculty of Science and Technology

Institute of Technology

**Autonomous motion planning for spacecrafts near small solar system
bodies: simultaneously refining the gravitational field model and
re-planning gravity dependant maneuvers**

Aditya Savio Paul

Master's thesis (30 EAP)

Robotics and Computer Engineering

Supervisor(s):

Dr. Michael W. Otte

Dept of Aerospace Engineering
University of Maryland, College Park
United States of America

Mr. Viljo Allik

Tartu Observatory
University of Tartu
Estonia

Tartu, Estonia 2020

Dedicated to my grandparents and parents

Contents

List of Figures	5
List of Tables	7
List of Algorithms	7
Abbreviations and Nomenclature	8
Resümee/Abstract	12
1 Introduction	13
1.1 Motivation	14
1.2 Road map	14
2 Background and Related Study	15
2.1 Small Solar System Bodies	15
2.1.1 Asteroids	15
2.1.2 Comets	15
2.1.3 Planetoids	15
2.2 Gravity Measurements	16
2.3 Motion Planning	17
2.3.1 Sampling-based planners	17
2.3.2 Motion Planning for spacecraft systems	19
3 Problem Statement(s)	20
3.1 Exploring viable way-points	20
3.2 Measuring gravitational attraction	22
3.3 Simultaneously updating gravity model and re-planning maneuvers	23
3.4 Cost Function	24
3.5 Objective Function	24
3.6 Constraint Function	25
3.7 Objectives	25
4 State of the Art	26
4.1 Software Resources	26
4.2 Experimental Approaches	26

5	Methodology	27
5.1	Gravity Field Model	28
5.2	Motion Planner	29
5.2.1	Algorithm Development	31
5.3	Simulation Environment	34
6	Experimentation and Analysis	35
6.1	Study 1 : Asteroid Eros 433	35
6.1.1	About	35
6.1.2	Experimental Outcomes	35
6.1.3	Result Analysis	39
6.2	Study 2 : Binary SSSB System	40
6.2.1	About	40
6.2.2	Experimental Outcomes	40
6.2.3	Result Analysis	44
6.3	Study 3 : Contact Binary System	45
6.3.1	About	45
6.3.2	Experimental Outcomes	45
6.3.3	Result Analysis	49
7	Further Contributions	50
8	Conclusion	51
	Bibliography	53
9	Appendices	59
	Study : False positive	59
	VEctor Gravimeter for Asteroids (VEGA)	60
	Keplerian Orbital Parameters	61
	Sphere of Influence (SOI)	62
	Software Information and Associated Libraries	63
	Hardware Specifications	63
	Non-exclusive license	64

List of Figures

2.1	Small Solar System Bodies	15
2.2	Gravity models for Earth, based on GRACE data	16
2.3	Sampling-based approach to path planning	17
2.4	Randomly Exploring Trees	17
2.5	Randomly Exploring Trees Star (RRT*)	18
5.1	Motion planning space definitions	27
5.2	Gravitational Acceleration exerted by a uniform body in an elliptical orbit . . .	28
5.3	Trajectory model control for receding time horizon approach	29
5.4	Trajectory optimization and model control over succeeding explorations	30
5.5	Small solar system body as mass concentration model	34
5.6	Simulation Environment developed on Visual Python and WebGL	34
6.1	Initial path plan estimate around Eros 433 in the earth-based gravity field model	36
6.2	Simulation environment : exploration at a distance of 50 km from Eros 433 Asteroid	36
6.3	Updating Gravity field model during orbital exploration around Eros 433 asteroid	37
6.4	Trajectory points for spacecraft motion at different exploration points within an orbit of 50 km from Eros 433 Asteroid with continuous updating of field model and refining orbital maneuvers	38
6.5	Visual Comparison of Earth-based (left) and In-Orbit (right) Gravitational Acceleration Model after 7 orbital maneuvers at a distance of 50 km	39
6.6	Thrust analysis for orbital motion for Asteroid Eros433	39

6.7	Initial path plan estimate around A in the earth-based gravity field model at a distance of 30 km (rotated 90°CW)	41
6.8	Simulation environment of exploration within halo orbit for B at a distance of 30 km from A	41
6.9	Updating Gravity field model during orbital exploration around Asteroid A . . .	42
6.10	Trajectory points for spacecraft motion at different exploration points within an orbit of 30 km from SSSB A with continuous updating of field model and refining orbital maneuvers (rotated 90°CW)	43
6.11	Visual Comparison of Earth-based (left) and In-Orbit (right) Gravitational Acceleration Model after 13 orbital maneuvers at a distance of 30 km	44
6.12	Thrust analysis for orbital motion for SSSB	44
6.13	Initial path plan estimate around SSSB in the earth-based gravity field model at a distance of 100 km	46
6.14	Simulation environment of exploration at a distance of 100 km	46
6.15	Updating Gravity field model during orbital exploration around SSSB	47
6.16	Trajectory points for spacecraft motion at different exploration points within an orbit of 100 km from SSSB with continuous updating of field model and refining orbital maneuvers	48
6.17	Visual Comparison of Earth-based (left) and In-Orbit (right) Gravitational Acceleration Model after 19 orbital maneuvers at 100 km	49
6.18	Thrust analysis for orbital motion for SSSB	49
9.1	False positive study where the spacecraft flies out of orbit in absent gravity zone	59
9.2	VEctor Gravimeter for Asteroids	60
9.3	Graphical Representation of Keplerian Parameters	61
9.4	Sphere of Influence	62

List of Tables

5.1	Key frames for Gravity Field Model	28
6.1	Specifics about Eros 433 Asteroid	35
6.2	Specifics about SSSB A and its moon B	40
6.3	Specifics about Contact binary SSSB	45
9.1	Specifics about VEGA Instrument	60
9.2	Software and Library information	63
9.3	Hardware Specifications	63

List of Algorithms

1	Randomly exploring tree algorithm	21
2	Rapidly exploring Randomly Tree Algorithm over viable way-points	21
3	Way-point exploration and motion planning	31
4	Gravity measurement and mapping	32
5	Simultaneous Motion Planning and Mapping	33
6	Spacecraft Orbit Visualization	33

List of Abbreviations

BIOS	Basic Input Output System
BVP	Boundary Value Problem
CPU	Central Processing Unit
DARPA	Defence Advanced Research Projects Agency
DoF	Degrees of Freedom
DRC	Darpa Robotics Challenge
EGM	Earth Gravity Model
GB	Gigabytes
GFM	Gravity Field Model
GGM	GRACE Gravity Model
GHz	Gigahertz
GMAT	General Mission Analysis Tool
GRACE	Gravity Recovery and Climate Experiment
HDD	Hard Disk Drive
HTML	Hypertext MarkUp Language
IDE	Integrated Development Environment
IDLE	Integrated Development and Learning Enviroment
IMU	Inertial Measurement Unit
JGM	Joint Gravity Model
MAT	Multi Asteroid Touring
NASA	National Aeronautics and Space Administration
NEAR	Near Earth Asteroid Rendezvous
OS	Operating System
PANGU	Planet and Asteroid Natural Scene Generation Utility
PRM	Probabilistic Road Map
RAM	Random Access Memory
RDT	Rapidly Exploring Dense Trees
ROS	Robot Operating System
RRT	Rapidly Exploring Random Trees
RRT*	Rapidly Exploring Random Trees Star

SBP	Single Body Problem
SDK	Software Development Kit
SLAM	Simultaneous Localisation and Mapping
SOI	Sphere of Influence
SSD	Solid State Drive
SSSB	Small Solar System Bodies
SST	Spatially Exploring Sparse Trees
TB	Terrabytes
TM	Trade Mark
UHD	Ultra-High-Definition
VEGA	VEctor Gravimeter for Asteroids
VPython	Visual Python
WebGL	Web Graphic Library

List of Nomenclature

Motion Planning

$\bar{\lambda}_i$	Way-point list of auxiliary randomly explored nodes
\bar{G}_f	Real-time gravity model
\bar{L}	Auxiliary way-point list
\bar{O}_i	Near optimal nodes during exploration
Δt	Minimum time of exploration
Γ	Trajectory function
\hat{r}	Direction vector
Λ	Objective Function
λ_i	Way-point list of randomly explored nodes
$\langle T \rangle$	Trajectory generated over viable way-points
\mathbb{G}	Ground truth gravity
\mathbb{M}	Motion planner
\mathbb{S}	Free space
ω	Argument of Periapsis
r	Reference model
u	Measured values
v	Velocity of spacecraft
ξ	Orbital influence
C	Configuration space
C_{free}	Free configuration space
C_{obs}	Observed configuration space
dv	Minimum distance between consecutive nodes
F	Gravitational force of attraction
G	Gravity model
G_f	On-board gravity model
H	Heuristics
i	Current iteration
J	Cost function

L	Way-point list
m_1	Mass of smaller body
m_2	Mass of larger body
N	Total iteration
n_v	Number of vertices of exploring tree
O	Way-point list of optimal nodes
O_i	Optimal Nodes during exploration
O_{aux}	Auxiliary node
O_{goal}	Goal node
O_{init}	Initial node
O_{near}	Nearest randomly explored node
O_{new}	Latest randomly explored node
O_{opt}	Optimal explored node
O_{rand}	Randomly explored node
V	Gravitational potential
v_f	Final velocity
v_i	Initial velocity
w_u	Weight of measured values
w_x	Weight of initial model
x	Initial model
r	Distance between two bodies
r_{SOI}	Radius of sphere of influence
t_o	Present time

Space Technology

γ	Reference direction
ν	True Anamoly
Ω	Right ascension of ascending node
a	Semi major axis
i	Inclination
e	eccentricity
M	Mean Anamoly

Constants and Units

au	Astronomical Unit : $1.496 \times 10^8 \text{ km}$
G	Gravitational constant : $6.67408 \times 10^{-11} \text{ m}^3\text{kg}^{-1}\text{s}^{-2}$
K	Kelvin
kg	Kilogram
km	Kilometer

Resümees/Abstract

Autonoomne trajektoori planeerimine väikeste taevakehade läheduses: jooksev gravitatsioonivälja mudeli täiendamine ja orbitaalmanöövrite ümberplaneerimine

Väikseid taevakehasid on võimalik paremini uurida neid ümbritsevatelt orbiitidelt. Orbiidi trajektoori arvutamine ja manöövrite planeerimine väikeste taevakehade ümber on aga keerukas nende nõrga ja ebakorrapärase gravitatsioonivälja tõttu. Maalt sooritatud kaugvaatluste põhjal planeeritud orbitaaltrajektooriid on aga tavaliselt ebatäpsed ning ei arvesta taevakeha vahetus läheduses sooritatud mõõtmistega.

Orbiidi trajektoori jooksev planeerimine võimaldab väikseid taevakehasid paremini uurida. Täpne orbiidi trajektoori planeerimine eeldab täpset gravitatsioonivälja mudelit, mida on võimalik kaardistada taevakeha mõjusfääris. Gravitatsioonivälja mudeleid analüüsides on võimalik hinnata taevakehade koostist ja massi jaotust.

Käesoleva töö raames töötati välja meetod, mis täpsustab missiooni käigus jooksvalt gravitatsioonivälja mudelit ja uuendab planeeritud orbitaalmanöövreid. Väljatöötatud meetod võimaldab satelliidil autonoomselt sooritada orbitaalmanöövreid, valida maandumispaika ning hinnata ressursside jaotust kohapealseteks mõõtmisteks.

CERCS: T125 -Automaatika, robotika, juhtimistehnika T320 - kosmosetehnoloogia [1]

Märksõnad: liikumise kavandamine, taanduv silmapiir, kosmosetehnoloogia, gravitatsioon

Autonomous motion planning for spacecrafts near small solar system bodies: simultaneously refining the gravitational field model and re-planing gravity dependant maneuvers

Small solar system bodies can be better studied while orbiting in their vicinity. However, orbital motion around such bodies is challenging due to their irregular and weaker gravity as compared to larger bodies. Moreover, *a-priori* paths developed by earth-based measurements tend to generate monolithic trajectories. Dynamic path planning in space has the potential to improve the study of small solar system bodies. Fine-grained motion plans require detailed knowledge of the gravitational forces, that can be measured in the sphere of influence. The gravity models can be analysed for mass and material distribution across the body.

We propose a method for autonomous motion planning around small solar system bodies that simultaneously measures and refines the gravitational model. The trajectories are re-planned considering the updated model to perform stable orbital maneuvers eventually providing a high fidelity gravity model. The research shall enable the spacecraft to perform autonomous maneuvers, design landing strategies and scout for in-situ resources.

CERCS: T125 - Automation, robotics, control engineering; T320 - Space technology [1]

Keywords: motion planning, receding horizon, space technology, gravity.

1 Introduction

The presence of small solar system bodies (*SSSB*) has sparked our curiosity to research about their creation, trajectories and resources they house. In near-present times, these bodies are being studied extensively by earth-based observations through instruments that continuously record data based on math models and estimations. These observations include orbital properties like trajectory and velocity; physical properties like albedo, volume and gravitational influence.

The knowledge of the gravitational field of these bodies is essential. The gravity field model of the *SSSB* can be interpreted to relay information like mass-density distribution and, to a certain extent, the material composition of the body as well. However, as compared to larger bodies in space, the force of gravity exerted by these bodies is magnitudes smaller and more distributed, owing to their irregularity and composition. Earth-based measurements generate low fidelity models of these bodies and do not accommodate the smaller gravitational forces that the body may exert thus missing out on relevant information about material distribution and composition. To obtain detailed field models, measurements are to be made in their vicinity that requires in-orbit maneuvers. Even so, in-orbit measurement becomes a challenge because of the erratic gravitational forces of attraction that the orbiting spacecraft might experience. Such irregular gravity fields host a dynamic environment that require advanced motion planning techniques for the spacecrafts to be able to re-plan trajectories based on it's location and understanding of the environment.

Thus, there is a need to plan the motion of the spacecrafts in way that dynamic trajectories are developed by updated knowledge of the gravitational forces experienced by it. This works by simultaneously measuring the gravitational attractions and updating the on-board gravity field model. The motion planning would also provide a highly defined field model of the gravitational forces exerted by the *SSSB* as compared to earth-based gravitational measurements.

Our research focuses on utilizing the dynamic gravity field of the *SSSB*, to perform near-real time path planning for orbital maneuvers. The trajectories are planned with the intention to refine the gravity field map as quickly as possible and achieving a stable orbital motion. We use a receding horizon approach. During each planning epoch, the planner considers the gravitational influence over a tree of orbital maneuver sequences (between discrete points in the orbit). Way-points are explored over sparsely-expanding geometric random-trees. Starting with the (low fidelity) gravity model created from earth-based observations, the gravity model is continually updated during the mission as the spacecraft experiences varying gravitational forces. On-board instruments measure the experienced forces observed by the craft eventually providing a high-fidelity gravity field model of the body. The updated model is simultaneously and continually used to re-plan the craft's trajectory during the mission, ensuring that each maneuver respects the most up-to-date model of the body's gravity field. Such an approach has the potential to contribute to autonomous spacecraft maneuvers, flybys and surface landings missions.

1.1 Motivation

Research has shown that small solar system bodies house materials that can advance our knowledge about the creation of the universe and support human life beyond earthly resources with fuel and building material. The research is motivated by the fact that small yet considerable measurements relating to gravity field distribution can be accomplished by in-orbit exploration. The high fidelity models accommodating larger and smaller forces of attraction can be analyzed to predict topographical aspects and material distribution across the surface of the SSSB.

Research and development into space exploration has advanced simulation-based mission planning approaches to predict the location of SSSB and plan missions to explore them[2]. These simulations, progress as experiences that probable succeeding outcomes of orbital explorations.

This thesis addresses the development of a novel motion planning technique to perform stable maneuvers in the gravitational sphere of influence of the SSSB by using the attractive forces exerted on the orbiting spacecraft and re-planning succeeding maneuvers.

1.2 Road map

The spacecraft trajectory is realized by kino-dynamic ¹ motion planning using sparsely-exploring trees with a receding horizon approach. The work is directed by four milestones:

- To realize an initial path plan for the spacecraft based on earth-based gravity field model.
- Measure and update the gravitational influence to the on-board model.
- To respect the updated gravity model in re-planning orbital maneuvers, attempting to achieve a stable orbital motion.

¹Kino-dynamic : motion planning problem that deals with boundary conditions of velocity and acceleration within force and torque constraints

2 Background and Related Study

2.1 Small Solar System Bodies

Small Solar system bodies[3] in fig 2.1 as defined by the International Astronomical Union [4] comprise of asteroids, comets and planetoids that majorly populate orbits around Jupiter[5] and Neptune[6]. These bodies seem to have chipped off from the surface of larger bodies or failed to have co-joined with other bodies in forming bigger bodies [7]. In either case, the SSSB have interested us to research about formation and material composition.

2.1.1 Asteroids

Asteroids [8] are mostly rocky and dry. They are studied by radiometric processes and in-orbit observatories that map their surface characteristics along with albedo, gravitational influence, dimensions etc. Asteroids like Eros433 explored by the NEAR mission [9] and Ida, have been studied extensively.

2.1.2 Comets

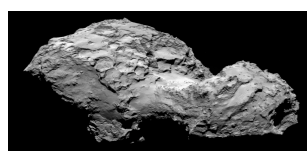
Comets [10] generally possess an icy surface as they tend to be present at a much larger distant from the sun. Their motion leaves a trail of residual dust, that is termed as the ‘tail’ of the comet and contributes to the study of the direction and the material composition of the comet. Halley’s, 103P/Hartley, 322P/SOHO [11] are some of the observed comets.

2.1.3 Planetoids

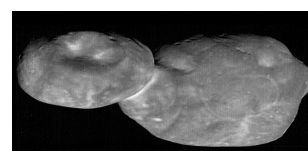
Planetoids [12] are usually referred to bodies that are slightly larger than the generic asteroids however the definition remains undefined(2019). They are synonymous to minor planets owing to their size. Ultima Thule (2.1c) has been designated as a minor planet when it was first observed by the New Horizons mission [13] in the Trans- Neptunian orbit.



(a) Eros 433 Asteroid [14]



(b) Rosetta Comet [15]



(c) Ultima Thule [16]

Figure 2.1: Small Solar System Bodies

2.2 Gravity Measurements

Gravity as defined by Sir Issac Newton in his ‘Theory of Universal Gravitation’[17], is the force exerted by a body on another body by virtue of its mass and relative distance between their centres.

This definition has been very useful in measuring and mapping the gravitational field of large bodies like planets. The GRACE experiment [18] consists of a system of two satellites, Tom and Jerry. The measurements are performed by the principle of the change in distance between the two satellites. Whenever one satellite experiences a gravitational anomaly, the other records the change in distance between the two. This causes a change in acceleration values that are recorded. By correlating these trends with the location provided by global positioning system(GPS) satellites, a gravity model of the earth is generated. These maps are developed under different conventions like Joint Gravity Model (JGM) and Earth gravity Model (EGM). Plots in figure 2.2 show a spatially distributed gravity field model of the earth generated over the EGM and JGM from the GRACE data.

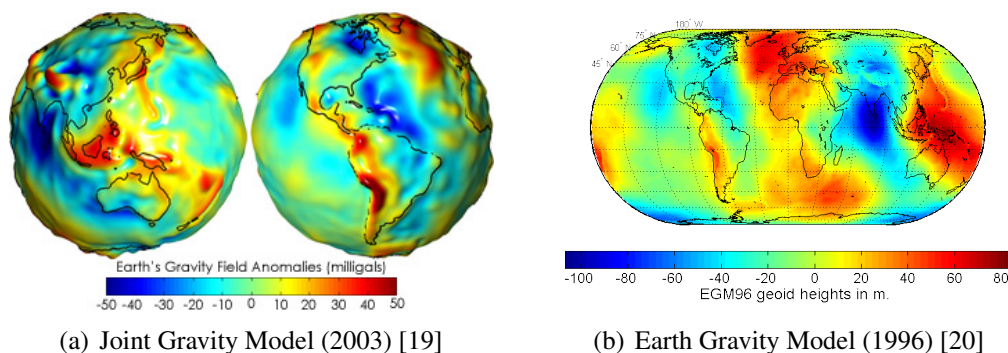


Figure 2.2: Gravity models for Earth, based on GRACE data

Earth-based experiments to measure gravity fields of other celestial bodies are performed by radiometric instruments that measure the dissemination of material surface of the bodies along with the rate of change position. Additionally, the gravitational affect on other nearby objects like moons and smaller rocks is also studied. Subsequent energy levels signatures can also be mapped as per Yarkovsky effect [21] [22], wherein the heat released from the surface of the bodies provides a certain thrust to the motion of the body[23]. Some measurements are also asserted by the apparent anatomy of the rocks. However, missions like Near Earth Asteroid Rendezvous(NEAR) [24] [25] [26] and the Hayabusa [27] provide insights into the gravity field as the spacecraft experienced forces, within the field of influence. These missions offer high-fidelity data than earth-based observations.

Instruments designed to measure gravity are gravimeters. They are located within specific positions in the spacecrafts that isolate the motion of the craft from the accelerometer to provide readings of induced acceleration by gravity. Ever since the development of the gravimeter by LaCoste and Romberg in 1936, the technology has modernised terrestrial mapping as well as precise mapping of gravity fields for smaller bodies like asteroids and comets. Carroll and Faber [28] described a novel technique to measure the gravity field of a small body by using the gravity gradient measured with a bias-free accelerometer. Hence in-orbit gravity measurements are considered to provide accurate gravitational data measurements as compared to earth-based measurements.

2.3 Motion Planning

2.3.1 Sampling-based planners

Sampling-based algorithms like probabilistic road map (PRM) (Kavarki [29]) and rapidly exploring random trees (RRT) (LaVelle [30]) develop paths over way-points in the configuration space. This lay the foundation to explore trajectories explored by random sampling, quasi-random sampling and n-query mapping.

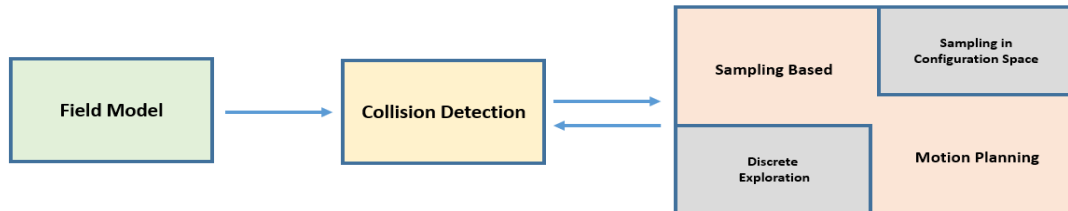


Figure 2.3: Sampling-based approach to path planning by LaVelle[30]

Sampling-based planners that use tree-based explorations of the configuration space (figure 2.5)[31] have the capability to solve n-boundary value problems (BVP) in a dynamic environment by randomly sampling in the configuration space [32]. The trees do so, by also considering the collision space (figure 2.3 [30]) and danger space to plan and execute a safe trajectory.

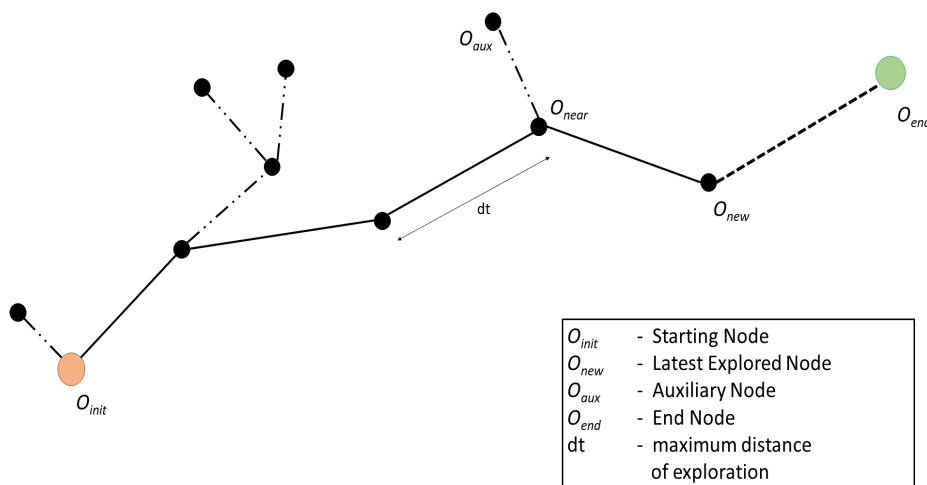


Figure 2.4: Randomly Exploring Trees (based on concept by LaVelle[30])

As research with tree-base planners progressed, rapidly exploring random trees star (RRT*) introduced almost sure asymptotic optimality ¹ [33] to path planning. The approach to optimal path planning over sampling-based algorithms provided a cost-efficient strategy to reach the goal state based on updated field model– by re-sampling nodes, from the latest iterations rather than re-planning from the initial node within the tree.

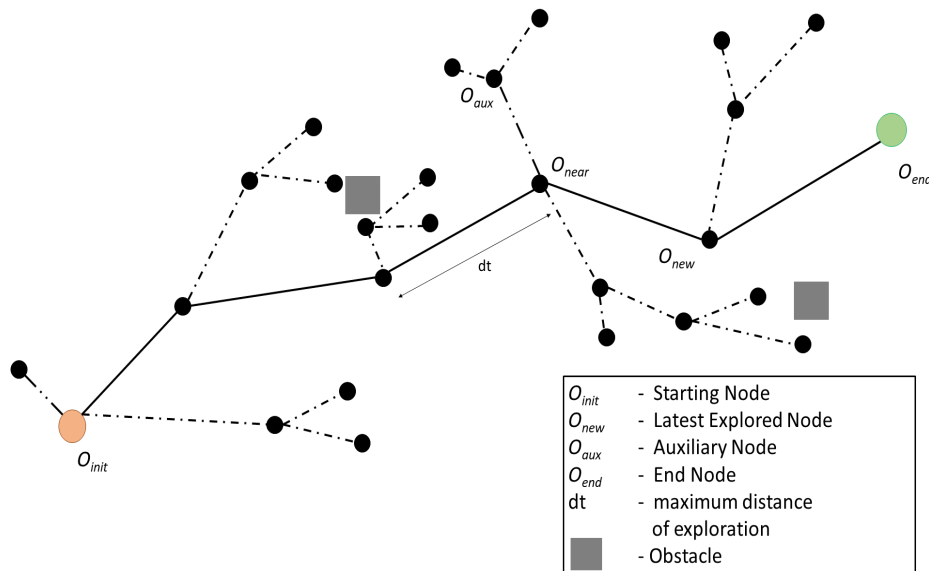


Figure 2.5: Randomly Exploring Trees Star (RRT*)
(based on work by Naderi et al.[34])

Research conducted by Otte and Frazzoli [35] modelling a dynamic environment with un-predicted obstacles, used an asymptotically optimal single-query algorithm to solve the dynamic motion planning problem. Erratic environments can be modelled within the algorithms to plan active maneuvers. The real-time updated knowledge of the environment is acknowledged to execute motion, based on the defined constraints.

In 2016, Li Y et al. introduced the concept of sparse RRT [36] that defined the premise of kino-dynamic path planning in configuration space, which was based on RRT and RRT* motion planning approaches. Sparse RRT was established as a near-optimal sample-based path planning algorithm that explored nodes asymptotically to converge faster paths by maintaining only a sparse set of samples. This made the algorithm computationally efficient over other algorithms for real-time dynamic motion planning of robotic motion. This concept later showed dynamic path planning approaches within a sparse data structure for answering path queries to improve the possibility of feasible solutions with computational efficiency. Based on asymptotically near-optimal approach for a kino-dynamic motion planning problem developed for a cost function J with finite cost J^* , the probability that the algorithm will find a solution of cost $J < tJ^*$ for some factor $t \geq 1$ converges to 1 as the number of iterations approaches infinity.

¹Optimal solution is a definition of the problem statement that correlates to a convenient state which is as close as to the ground truth. It is defined as the best solution for the given set of the constraint and field information. Asymptotic optimality tends to correlate to the ground truth with a near-infinity probabilistic solution

A receding horizon approach to estimate a path generation was demonstrated by Tsiotras and Panagiotis [37] in 2006 for a wheeled autonomous vehicle traversing at very high speeds for a predicted control model. The research tackled a single constraint velocity optimization with the derived acceleration limits without considering the distance. It was analysed by Worthmann, 2011 [38] that a constrained receding horizon ² outperforms an unconstrained approach for a non-linear system.

2.3.2 Motion Planning for spacecraft systems

With the immense possibilities that space exploration offers, the research for advanced techniques that can explore the bodies in space, is needed. This has elevated interest in spacecraft and satellite autonomy to safely approach and orbit the body in space for further study. The discipline introduces extensive research in the field of path planning algorithms from terrestrial to extra-terrestrial applications. There have been a plethora of papers and research published that advance motion planning for ground and aerial robotic systems.

The notion of satellite autonomy as explored by Golden [39] states the requirement of dexterous motion plan in space using state-of-the-art technological readiness. In 2002, Richards et al. [40] worked on trajectory planning using mixed-integer linear programming for satellite maneuvering. However, it did not dictate optimal path planning. In 2007, Dario and Lorenzo [41] introduced autonomous and distributed motion planning for satellites in a swarm ecosystem by inverse dynamic calculations for equilibrium sharing. The research concentrated on the pre-planned formation of the multi-agent system and did not accommodate for a dynamic approach in state space to plan a real time path for the satellites.

An approach to define spacecraft motion during mission execution was explored by [42] in 2011 within initial and final constraints. The problem was solved by heuristics ³ within Clohessy-Wiltshire equations by Hablani and Tapper [43] by defining relative navigational for approach and exit algorithms within a circular orbit. Lopez and McLnnes [44] sought the approach to autonomous rendezvous using artificial potential field guidance however the feasibility of proximity operations was quite low for the same. Close proximity missions for small bodies in the solar system require high dexterity within the spacecraft and robotic system.

M.Pavone at the Stanford University working on algorithmic foundations for real time spacecraft motion planning [45], studied the methodology of randomly exploring dense trees to plan in dynamic environment near these small bodies. The results were tested to be near-sighted on the space robotics test bench to illustrate the feasibility of the approach. With these advancements and the curiosity to explore small bodies in space, that host an inherently dynamic environment, it has become the need of the hour to develop path planning approaches for spacecrafts to study from in-orbit exploration. Apart from space debris in the path of the spacecraft trajectory, another prominent dynamic environment offered by the small bodies are their relatively low force of gravitational within their influence. The knowledge of the gravitational field is essential for planning spacecraft maneuvers in the influence of the body to perform in-orbit experimentation.

²Horizon, within the robotics community, is defined as the state space up-to which a series of way-points are explored to develop trajectories. In this research, the configuration space is explored over geometric trees for every epoch and the time taken is considered to be a single event horizon.

³Heuristics employ a practical approach to solve a problem statement over a given set of conditions. They are used as a positive catalyst to reach an optimal or stable solution within a reasonable time frame. Heuristic based examples include a logical assertion, educated guesses and common sense

3 Problem Statement(s)

The problem considered in this research is active re-planning of spacecraft trajectory within the sphere of influence (*SOI*) of SSSB. This is done by realizing the attractive forces, experienced by the spacecraft and utilizing the knowledge to plan future maneuvers.

The first problem attempts to develop the trajectories over viable way-points within the free space and restrict the spacecraft – either from getting too close or too far away. These constraints have been detailed in section 3.6.

The second problem maps the gravitational field at every point that the spacecraft traverses (section 3.2). These points of measurements improve the overall knowledge of the gravity field during orbital motion of the spacecraft by the same position or near-by positions in subsequent maneuvers.

The final problem solves simultaneous motion planning of the spacecraft while continuously updating the gravity field and re-planning the trajectories using the gravitational field (section 3.2). It is essential that every motion is carried out with respect to the recent gravity model.

3.1 Exploring viable way-points

The research direction intends to establish a motion planning approach to propose a path plan in the known gravitational field acquired from earth-based measurements field. The path is progressed autonomously as the gravity field model is updated by measuring the forces acted upon the spacecraft. Using a sampling-based planning approach [46], the definition regards the configuration space that is defined for the entire simulation environment.

For a configuration space C , to explore in the free space $C_{free} \subseteq C$, the spacecraft traverses over a trajectory $\langle T \rangle$ where no collisions occur. The explored way-points in the C_{obs} that satisfy the constraints, are used to develop trajectories.

The nodes are explored within a sparsely exploring tree-based topology, for a finite horizon. The trajectory is developed over the optimal way-points extending from a present state o_{init} to a future goal state o_{goal} . The topology ensures that the nodes are randomly explored, however only the viable nodes that lie within the heuristics defined as $C_{obs} \subset H(O)$, are considered. The algorithm to explore over rapidly exploring trees by LaVelle [30] is shown in Algorithm 1

Algorithm 1: Randomly exploring tree algorithm

```
For  $C$  with number of vertices  $n_v$  in distance  $dv$ ;  
 $C$ .init( $o_{init}$ );  
while  $C$  in  $n_v$  do  
   $o_{rand} \leftarrow$  RAND_CONF  
   $o_{near} \leftarrow$  NEAREST_VERTEX()  
   $o_{new} \leftarrow$  NEW_CONF( $o_{near}, o_{rand}, dv$ )  
   $C$ .add_vertex( $o_{new}$ )  
   $C$ .add_edge( $o_{near}, o_{new}$ )  
  Build Tree L  
return L ;
```

An initial path plan is executed based on the trajectory developed by the earth-based measurements. Succeeding trajectories are executed as in-orbit gravity is measured. For every new gravity measurement, the subsequent gravitational accelerations is updated on the on-board field model. Since algorithm 1 does not produce a near-optimal solution, it is required that the set of nodes or way-points are considered over a set of constraints defined within the heuristics, that are considered to develop a trajectory that complies with the problem statement. Algorithm 2 is a heuristic-based approach to determine the viable nodes within the exploration and then consider the same for path planning. Eventually, the continuous mapping and updating of the gravitational field to reach a stable orbit advances the spacecraft trajectory model from *a-priori*¹ state to a *posteriori*² state within the defined constraints in the configuration space.

Algorithm 2: Rapidly exploring Randomly Tree Algorithm over viable way-points

```
For  $C$  with number of vertices  $n_v$  in distance  $dv$ ;  
 $C$ .init( $o_{init}$ );  
while  $C$  in  $n_v$  do  
   $o_{rand} \leftarrow$  RAND_CONF  
   $o_{near} \leftarrow$  NEAREST_VERTEX()  
  if  $H(o_{near}) \sim True$  then  
     $o_{opt} \leftarrow o_{near}$   
  else  
     $o_{aux} \leftarrow o_{near}$   
   $o_{new} \leftarrow$  NEW_CONF( $o_{near}, o_{rand}, dv$ )  
   $C$ .add_vertex( $o_{new}$ )  
   $C$ .add_edge( $o_{near}, o_{new}$ )  
  Build Tree L  
return L ;
```

¹*a-priori* - Knowledge obtained through analysis

²*posteriori* - Knowledge obtained through observation

3.2 Measuring gravitational attraction

The force exerted on a body by another body by virtue of its mass and the distance between their centers, is defined by the Newton's law of universal gravitation. It states that 'any particle of matter in the universe attracts any other with a force varying directly as the product of the masses and inversely as the square of the distance between them.' [47] [48] The concept of universal gravitation is mathematically expressed as

$$F = -G \frac{m_1 m_2}{r_{21}^2} \hat{r}_{21} \quad (3.1)$$

$$\hat{r}_{21} = \frac{\vec{r}_{21}}{|\vec{r}_{21}|} \quad (3.2)$$

where,

F : Force

G : Gravitational Constant

m_1 : mass of body 1

m_2 : mass of body 2

r : distance between the two bodies

\hat{r} : Direction vector

Every body in the universe exerts a force on another body within the region of gravitation field, which is described as the force exerted on an area, at any given point in space, per unit mass. This value is equivalent to the gravitational acceleration of the body and correlates to the gravitational sphere of influence of a celestial body (see appendix 9).

Mathematically,

$$V = \frac{W}{m} \quad (3.3)$$

Work done (W) for the force required for a particular displacement, hence the gravitational potential (V) at distance r can be written as :

$$V(r) = \frac{1}{m} \int_{\infty}^r F \cdot dr \quad (3.4)$$

using equation 3.4

$$V(r) = \frac{1}{m} \int_{\infty}^r \frac{Gm_1 m_2}{r^2} dr \quad (3.5)$$

and solving the integral we achieve

$$V = -\frac{GM}{r} \quad (3.6)$$

for a 3-Dimensional space with the body to be explored at

$$r = \sqrt{(x_1 - x_o)^2 + (y_1 - y_o)^2 + (z_1 - z_o)^2} \quad (3.7)$$

3.3 Simultaneously updating gravity model and re-planning maneuvers

For every new measurement, the motion planner \mathbb{M} considers the updated field knowledge \bar{G}_f to plan the next trajectories for way-point exploration in the configuration space C .

This involves simultaneously mapping of the gravity field during orbital maneuvers by on-board instruments that relay the data, to the field model. This simultaneous mapping of the gravity field and planning the next trajectory is coherent to simultaneous localisation and mapping (SLAM) however it considers the gravity field distribution around the SSSB. The planned trajectory however should comply with the control constraints defined in heuristics H . The trajectory is developed over a function as mentioned in equation 3.8.

$$\langle T \rangle = \mathbb{M}(G_f, O, C) \quad (3.8)$$

for every planning epoch, the model is to be updated as,

$$\bar{G}_f \xrightarrow{\text{cartesian}} G_f \quad (3.9)$$

Starting with a low-fidelity model, as explorations progress, the gravity model gets more detailed. Simultaneously, the receding horizon tends to a stable orbital motion.

Hence the motion plan should have the capability of executing the previous maneuvers with low level knowledge of the gravity field. It should also consider the updated values to execute a series of maneuvers to attain a stable orbit around the SSSB. For every spacecraft position that the gravity is measured, the values are updated on the on-board gravity field model as the latest measurements performed within the orbital maneuvers. The previous field model \bar{G}_f measured over multiple measurements of V is mapped and updated with the real-time measurements G_f . The orbital maneuvers continue over $\langle T \rangle$ as explorations progress and detailed model of the gravity is generated.

3.4 Cost Function

Every epoch considers the event horizon to re-plan the maneuver considering the updated model. The concept to approach a stable orbit pans over a receding horizon methodology where the cost function is minimised $J < \alpha J^*$ and $\alpha \geq 0$ converges to 0 as number of iterations approaches infinity. Equation 3.10 illustrates a general statement of the cost function that postulates a weighted squared error reduction; the cost function needs to be minimised as explorations further with time. A detailed cost function for the development of the experiment is mentioned in chapter 5.

$$J = \sum w_x(r - x)^2 + \sum w_u \Delta u^2 \quad (3.10)$$

where ,

- x : Initial Model
- r : Reference Model
- u : Measured Values
- w_x : Weight of x
- w_u : Weight of u

3.5 Objective Function

The representation of the objective function Λ is a definition of the optimization of the cost 3.4 and constraint function 3.6. This can be expressed as a continuous iterative process to reduce the cost function as we utilise a receding horizon approach by sampling random nodes within the finite event horizon.

The objective function for our approach takes into account, the initial point of exploration and is sparse over multiple nodes until the goal is reached. This is denoted as a weighted (w) sum of all iterations over minimizing the cost function.

$$\Lambda = \sum_{i=1}^N w_i \cdot \Lambda_i \quad (3.11)$$

The objective function defines the trajectory length maintain the distance between two consecutive nodes of exploration considering the velocity (v) of the spacecraft as -

$$\Lambda_1 = \sum_{i=1}^N \sqrt{(v_i)^2 + (v_f)^2} \quad (3.12)$$

where v_i is the velocity at initial node and v_f is the velocity at the goal node. This is penalised by a proximity to obstacle parametric approach with a minimum viable distance determined as

$$\Lambda_2 = \sum_{i=1}^N \left(\min\left(\frac{dv_i - o_i}{dv_i - o_{near}}\right) \right)^2 \quad (3.13)$$

3.6 Constraint Function

The constraint function ensures the motion constraints by realizing the obstacle space and the danger space (refer : figure 5.1).

The motion constraints enforce the spacecraft to maneuver within the limits of the escape velocity for the SSSB bounded between v_{min} and v_{max} with control limit as :

$$v_{i_{min}} < v_i < v_{i_{max}} \quad (3.14)$$

and the viable distance from the SSSB is reduced as

$$dv < dv_i - o_i < 0 \quad (3.15)$$

3.7 Objectives

Regarding the nature of the problem statement, the approach needs to be on-board and autonomous. For the given C that exists in the sphere of influence $C \exists \xi$, the randomly explored way-points need to lie in free space as $O \subset C_{free}$ defined by the objective function Λ . The trajectory ($\langle T \rangle$) is then developed over the free space C_{obs} by extending the tree $\langle T \rangle \xrightarrow{viable} O_{opt}$ from the current state to the goal state as $o_{init} \rightarrow o_{goal}$ of edge length dv .

The state space for the maneuvers is defined by the objective function Λ_2 to orbit at the desired distance. Every other way-point $o_{rand} \notin H$ is discarded. The trajectories that have been traversed are forgotten and the cost function J is minimised in order to improve sampling efficiency and trajectory optimization for the succeeding orbital maneuvers.

During this maneuver, the gravitational attractions are measured according to Equation 3.6 from the start state to the goal state and the on-board gravity model is mapped accordingly $\bar{G}_f \mapsto G_f$.

The on-board sensors and propulsion are assumed to deliver sufficient performance to execute the motion plan.

The approach is versatile to include more sensor models, and perform other experiments while establishing dynamic motion planning around the SSSB.

4 State of the Art

Motion planning for robotic systems has taken leaps and bounds with optimal planning strategies. Path planning in dynamic environments are developed on algorithms like rapidly exploring random trees and its variants ((RRT^*) , $(RRT\#)$, (SST)). They prove that efficient heuristic-based motion planning, considering kinematic constraints, improves real-time exploration.

Trajectory planning for spacecrafts has been evident since Apollo 11 (1969) landed on the moon. However, active maneuvering is eminent to explore the uncertain space environment. The Osiris-rex mission [49] to the 101955 Bennu is a sample-return mission that uses local visualization, simultaneous localization and mapping to estimate it's position and plan trajectories towards the landing site. The use-case of having highly optimized on-board navigation competency reduces the dependency on earth-based decisions hence gaining sufficient lead time.

Global challenges like DARPA Robotics Challenge [50] have encouraged development of dynamic path planning. Such practices optimize motion planning with the best utilisation of on-board resources.

4.1 Software Resources

Programming languages like MATLAB, Python and Julia can test hypotheses, develop algorithms and execute robotic motions. Open source projects like 'PythonRobotics' [51] [52] ¹ [53] provide insights to path planning approaches. [54]. Softwares like Kerbal Space Program, General Mission Analysis Tool (GMAT [55]) and PANGU [56], FreeFlyer [57] can execute space mission from the inception to the end of the life-cycle.

The estimated and actual mission data-sets have been essential in building these frameworks that aid us in planning missions to analyze possible scenarios. Frameworks and Libraries like Robotic Operating System (ROS), Python Orekit [58] provide the development kit to work with celestial conditions.

4.2 Experimental Approaches

Terrestrial, laboratory and in-orbit experiments provide the data to analyse the large-scale missions for spacecraft systems. In recent times, space-oriented company SpaceX successfully demonstrated their rocket-return procedure ² to provide re-usability of rocket systems, that provides insights to expand to celestial bodies as well, by dynamic trajectory optimization strategies. Failed experiments like the Chandrayan-1[59] also provide the essential insights to perform better initial calculations and assertions towards the actual missions. These experimental analyses, provide data that may be encountered during mission execution.

¹Python Robotics by Atsushi Sakai

²SpaceX Rocket Return Procedure - Source : TheVerge

5 Methodology

Motion planning for robotic systems is defined by a set of way-points that formulate a trajectory, estimate the path and execute the motion for the robot to navigate from one point to another in a determined or undetermined environment. The spacecraft with the motion plan on-board approaches the SSSB, with *a priori* initial information of the gravity field as measured from the Earth. Once in the influence of the gravity of the body, the spacecraft explores points within the orbit, while measuring the gravity and simultaneously updating the gravity field model to reconsider while planning the next orbital maneuvers. A sequence of valid configurations considering the configuration space, free space, target space, obstacle space, is planned, as illustrated in figure 5.1. Anything beyond the free space, is believed to be outside the sphere of influence of the gravitational pull of the SSSB and is considered as the danger space, while any space in extreme proximity to the SSSB is reasoned as the obstacle space.

The thrust exerted by the space for every maneuver is calculated and the change in the thrusting is plotted. A decrease in thrust is expected which is synonymous to the motion getting more stable as the on-board field model is updated.

The autonomously developed trajectories are based on the accurate measurement of the gravitational acceleration and precise location of the spacecraft. The on-board gravimeter [28] and propulsion systems are assumed to perform to the near-ideal expectations to justify performance viability. This section illustrates the modelling of the gravity field model, algorithm development and the simulation environment for the current research.

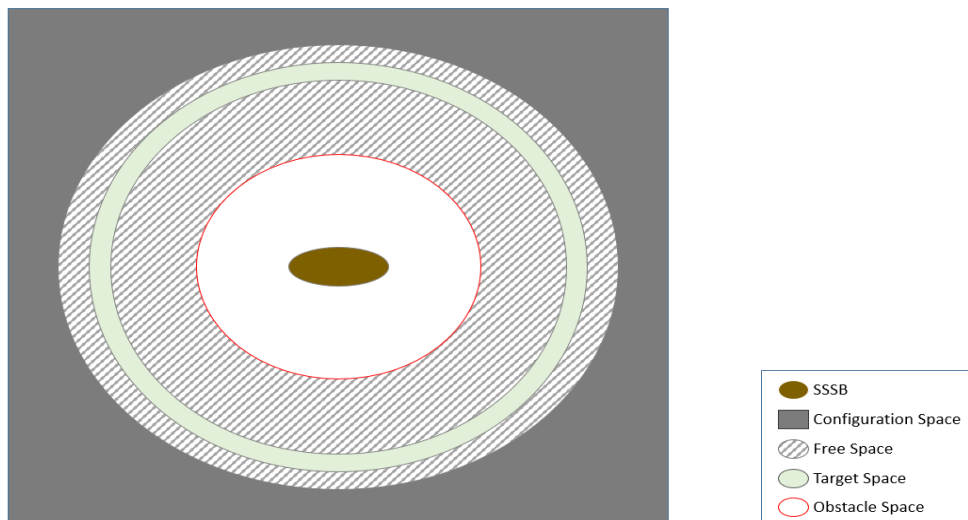


Figure 5.1: Motion planning space definitions

5.1 Gravity Field Model

Equation 3.6 gives a generalize foundation to the measurements that realize the measurement of the forces exerted by the bodies SSSB within their sphere of influence. The field models are generated as the potential at a particular distance from the centre of the SSSB with the spacecraft position in the cartesian coordinates. These models correlate to the measurements obtained from earth-based observations defined by Equation 3.1. The earth-based field model were the initial inputs to the motion planning algorithm (Algorithm 5). During actual maneuvers, the field model is updated with real-time measurements, while respecting the previous values. The algorithm identifies the key frames within the field model as illustrated in Table 5.1.

A general plot for gravitational distribution of a uniform body was generated and associated acceleration exerted by the body was plotted along over radial based and spatial interpolation of orbit distribution as depicted in figure 5.2.

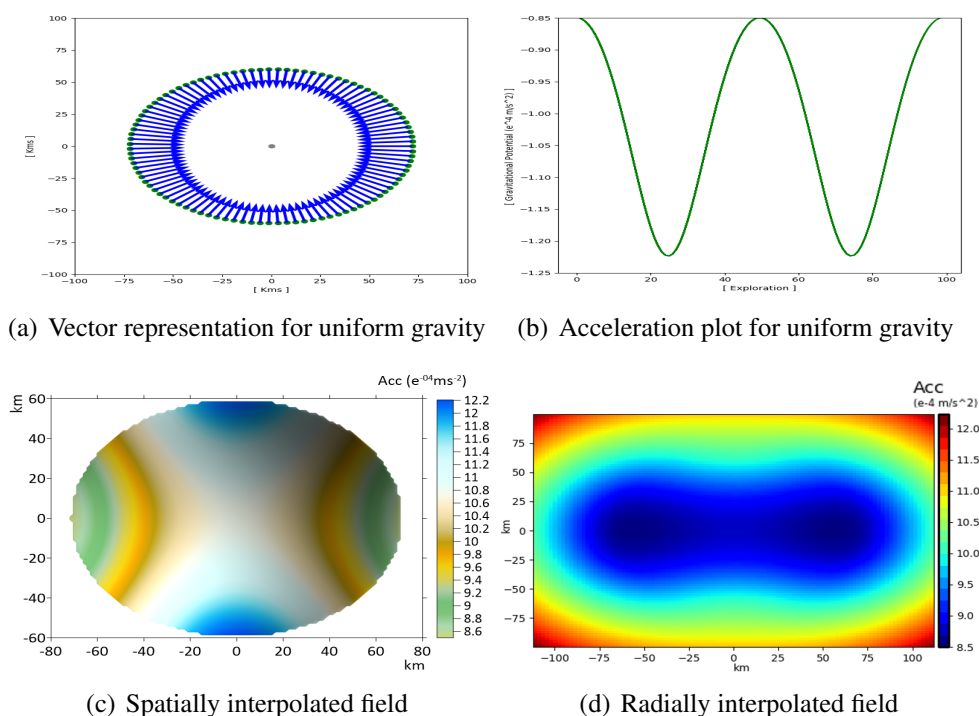


Figure 5.2: Gravitational Acceleration exerted by a uniform body in an elliptical orbit

X	Y	Z	Grav Acceleration ($m.s^{-2}$)
x_o	y_o	z_o	G_{a_o}
x_1	y_1	z_1	G_{a_1}
x_2	y_2	z_2	G_{a_2}
.	.	.	.
.	.	.	.
x_n	y_n	z_n	G_{a_n}

Table 5.1: Key frames for Gravity Field Model

5.2 Motion Planner

In our approach, the in-orbit maneuvers are used to explore various state trajectories from the current state to the next-future state, by randomly sampling the nodes within the constraints of distance and velocity. As the spacecraft navigates in the free space, a single-body problem is solved considering the spacecraft to be the only moving object. With each iteration, an optimization level is achieved which is not considered as final. As the exploration horizon keeps shifting forward to the sample the new space, near-asymptotic solutions are explored within the environment as the *posteriori* state.

A receding horizon approach for a sampling based motion plan is developed over sparsely-expanding trees. It realizes an iterative function over a finite horizon optimization within defined constraints while minimizing the cost. Each exploration is performed for a finite-time interval in the future represented as $[t_o, t_o + \Delta t]$. The control control algorithm uses the topology as illustrated in figure 5.3.

- Consider the initial field model to execute plan initial trajectory
- Perform real-time measurements update on-board gravity model
- Minimise cost function over control statements
- execute re-planned trajectory based on updated gravity model

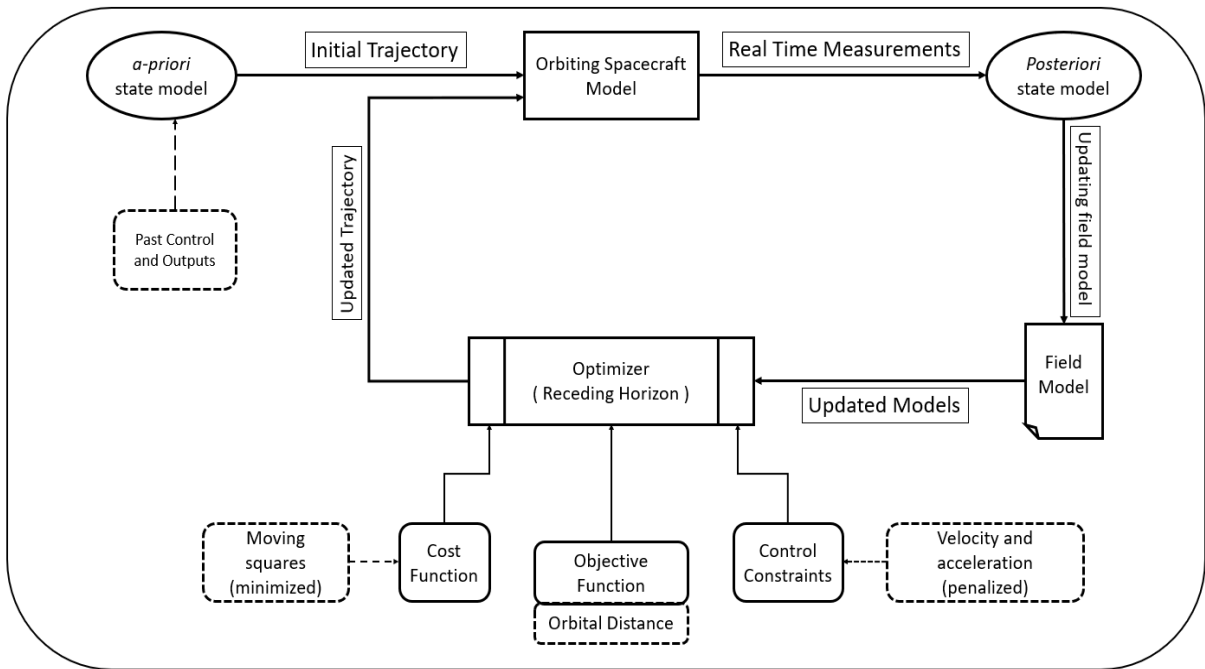


Figure 5.3: Trajectory model control for receding time horizon approach based on the concept illustrated by [60]

While maneuvering, the gravitational acceleration is measured spatially inwards between the centre of the spacecraft and the SSSB, assuming the SSSB to a continuous mass distribution. The heuristic (H) so defined in Equation 5.1 is a constraint of the velocity (v) and the distance (r) of the spacecraft from the centre of the small solar system body within the orbit of exploration.

$$H \forall f[v, r] \quad (5.1)$$

The cost function in equation 5.2 was modeled to solve the single body approach for the iterative exploration of nodes while attempting to minimize the cost function (J) over a period of spatial time exploration.

$$J = \sum_{i=1}^N w_{x_i} (r_i - x_i)^2 + \sum_{i=1}^N w_{u_i} \Delta u_i^2 \quad (5.2)$$

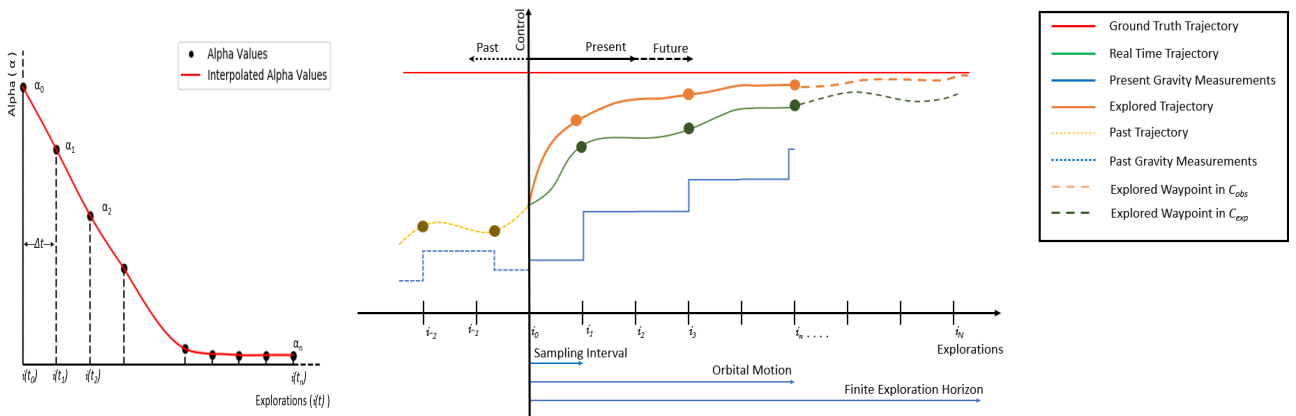
where,

- i : Current iteration
- N : Total iterations
- x : Initial gravity model
- r : Reference gravity model
- u : Measured gravity values
- w_x : Weight of x
- w_u : Weight of u

As shown in Fig 5.4a ([61]), the gradual decrease of the horizon can be observed. This is synonymous to the gravity model getting more and more detailed. The motion plan, reduces the cost function when it estimates lesser number of exploration are required to reach a viable solution between the predicted and the actual way-points of propagation.

Figure 5.4(b) shows the control model (Weng [62]) for the receding horizon motion plan. An initial trajectory is estimated based on the Earth-based measurements. Once in orbit, the model is updated with real-time measurements. The updated model is then used to re-plan the next maneuvers and tends to approach a stable solution. The trends represent the trajectory based on previous way-points which are forgotten over time, real-time trajectory based on explored way-points in explored configuration space and the explored way-points ahead of the current trajectory within the observed configuration space defined within the sampling intervals.

This exploring approach brings in a kino-dynamic motion planning within the orbital environment.



(a) Minimizing cost function

(b) Control model for receding horizon approach, concept taken from [62]

Figure 5.4: Trajectory optimization and model control over succeeding explorations

5.2.1 Algorithm Development

Way-point exploration and trajectory planning

The motion planner was based on the geometric trees concept of random exploration([34]). The trajectories were developed on the way-points that lie within the heuristics as defined by the control function and the objective function (see sections 3.6, 3.5). However, for algorithmic efficiency in the approach, the geometric trees explored sparsely. Only a sparse space was explored during maneuvers, viable way-points were saved, and the rest of way-points and the trajectories were forgotten.

A receding horizon method expanded the geometric trees in the target space to execute progressive stable maneuvers as the gravity field model became more and more detailed. For every way-point, where the gravitational pull exceeded the thrust to keep in the stable orbit, a way-point was explored that brought the spacecraft back to the designated distance of exploration. This required a higher thrust to be exerted by the spacecraft which was later analysed to have decreased with time.

According to the trajectory control model in figure 5.3, every orbital motion tended to be smoother as compared to the previous motion. However, the explorations progress with the assumption that the gravity within the sphere of influence was well defined. The Algorithm 2 illustrates a routine of the motion plan for every epoch. The time complexity for the trajectory optimization was $T(f) \in O(4)$ where ‘ f ’ is the explorations and ‘ O ’ is the worst case scenario.

Algorithm 3: Way-point exploration and motion planning

```

Define Orbital Influence  $\xi$  ;
Read earth-based gravity field model  $G_f$ ;
while True do
    free space extent  $\mathbb{S}_\xi$ 
    cost function  $J(G_f) \mid H$ 
    while iterations  $i$  in  $\mathbb{S}_\xi$  do
        while  $t$  in range  $[t_o, t_o + \Delta t]$  do
            | Sample random nodes  $\lambda_i$  ;
        end
        if  $\lambda_i \subseteq J \ \&\& \ \lambda_i \hat{=} H$  then
            |  $\lambda_i \mapsto$  Optimal Nodes  $O_i$  ;
            |  $\bar{\lambda}_i \mapsto$  Near Optimal Nodes  $\bar{O}_i$  ;
            Develop Trajectory  $\Gamma(\langle T \rangle \subset L)$  ;
            | Extend  $(L_{i-1} \dashv\circ L_i)$  ;
            while in  $L$  do
                | calculate  $E$ 
                | distance of SSSB between observed and explored way-points ;
            end
        end
        minimize  $J$  with  $\alpha_E$  ;
        return  $[\Gamma, \mathbb{S}_\xi^*, i]$  ;
    end
    forget  $O_i$  and  $\langle T \rangle$ ;
end

```

Measuring gravitational acceleration

For every spacecraft, the gravitational acceleration at the point was measured according to the math model detailed in equation 3.6. As the spacecraft moved on its trajectory, the gravitational acceleration was interpolated, between successive way-points by a radial based function (figure 5.2d).

This accounted for gravitational zone from the spacecraft to the SSSB, mapping a gravitational zone between the way-points. These updated forces were considered to further the trajectories which were slightly smoother than the previous ones. The gravitational acceleration were later plotted by spatially interpolating their values to visualise the changes in the gravity contour as in figure 5.2c. The time complexity for the gravity measurement was calculated to be $T(f) \in O(1)$.

Algorithm 4: Gravity measurement and mapping

```
Read on-board gravity field model  $G_f$ ;  
while in target space do  
    Sample random nodes  $\lambda_i$  ;  
     $\lambda_i \mapsto$  viable Nodes  $O_i$  ;  
     $O_i \rightarrow$  way-point list  $[L]$  ;  
    Measure gravity  $\tilde{G}_f$  at  $O_i$  ;  
    radially interpolate gravity  $O_{i-1} - O_i$  ;  
    Update  $\tilde{G}_f \mapsto G_f$  ;  
end  
return  $G_f$ 
```

Simultaneous motion planning and mapping of gravity field

For simultaneous motion planning and updating the gravity model, it was essential that the code worked well in real time.

With every update, the new gravity field model was respected to develop trajectories in the target space. The trees expanded according to the flow-logic in Algorithm 3 and the gravity was measured according to Algorithm 4. Simultaneously, these routines worked within the motion planner to execute the spacecraft trajectories, in the simulation environment.

Algorithm 5 illustrates the motion plan algorithm to realize the receding horizon approach for near-optimal exploration of nodes. The motion plan is visualised with Algorithm 6 within the simulation environment that hosts the spacecraft and executes the motion according to the motion plan developed in Algorithm 5.

Every epoch was considered within a time frame of less than 1 minute and individual maneuvers were executed within 0.1 seconds after the plan was generated.

With a time complexity of $T(f) \in O(f + f^3g)$, where ‘ g ’ is the epoch. The algorithm was executed for a hardware setup as mentioned in appendix 9.3. Test cases developed (chapter 6) illustrate the time of execution and lay the ideology of having an efficient flight controller for the autonomous motion and optimizing the algorithm for real missions.

Algorithm 5: Simultaneous Motion Planning and Mapping

```
Initialize motion planner  $\mathbb{M}$ ;  
Define Orbital Influence  $\xi$  ;  
Read on-board gravity field model  $G_f$ ;  
while True do  
  free space extent  $\mathbb{S}_\xi$   
  cost function  $J(G_f) \mid H$   
  while iterations  $i$  in  $\mathbb{S}_\xi$  do  
    while  $t$  in range  $[t_o, t_o + \Delta t]$  do  
      Sample random nodes  $\lambda_i$  ;  
    end  
    if  $\lambda_i \hat{=} G_f \ \&\& \ \lambda_i \subseteq H$  then  
       $\lambda_i \mapsto$  Optimal Nodes  $O_i$  ;  
       $O_i \rightarrow$  way-point list  $[L]$  ;  
       $\bar{\lambda}_i \mapsto$  Near Optimal Nodes  $\bar{O}_i$  ;  
       $\bar{O}_i \rightarrow$  auxiliary way-point list  $[\bar{L}]$  ;  
      Develop Trajectory  $\Gamma(\langle T \rangle \subset L)$  ;  
      Build Tree  $(L)$  ;  
      Extend  $(L_{i-1} \rightarrow L_i)$  ;  
      while in  $L$  do  
        calculate  $E$   
        distance of SSSB between observed and explored way-points ;  
      end  
    else  
       $\Gamma(\langle T \rangle \subset \bar{L})$  ;  
    end  
    Measure gravity  $\bar{G}_f$  at  $O_i$  ;  
    minimize by  $\alpha_E$   
    return  $[\Gamma, \mathbb{S}_\xi^*, i]$  ;  
  end  
  Update  $\bar{G}_f \mapsto G_f$  ;  
  forget  $O_i$  and  $\langle T \rangle$  ;  
end
```

Algorithm 6: Spacecraft Orbit Visualization

```
Initialize simulation environment ;  
Model SSSB and spacecraft ;  
while True do  
  Execute motion plan  $\mathbb{M}$  and measure thrust ;  
  Trail Spacecraft Path ;  
  Plot in-orbit values and gravity field heat map ;  
end
```

5.3 Simulation Environment

The algorithm was developed on the Python programming language and associated libraries mentioned in Appendix 9. The simulation environment was modelled in Visual Python(VPython), using the WebGL graphics library and related dependencies running on the local server. The environment hosts a small solar system body and the exploring spacecraft. The SSSB is a static body, rendered as a mass concentrated model (figure 5.5) and exerts the associated gravitational field. The astropy python library serves source of universal constants and the Sun is considered to be the center of the simulated environment.

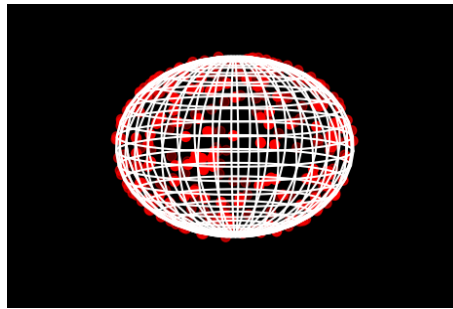


Figure 5.5: Small solar system body as mass concentration model

The spacecraft is considered to house a gravimeter [63] [64] that is adept in measuring the gravitational force exerted by virtue of change in acceleration and position. The propulsion provides the required thrust to execute the motion. The spacecraft's motion plan is executed in solving a single body motion problem.

The spacecraft trajectory was visualized in visual python and data was processed over python. The mission data was also stored as a database for post analysis.

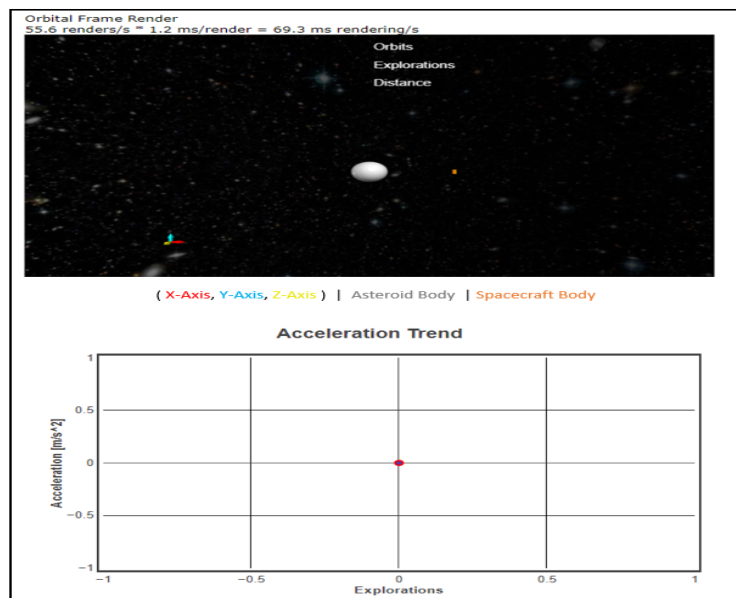


Figure 5.6: Simulation Environment developed on Visual Python and WebGL

6 Experimentation and Analysis

6.1 Study 1 : Asteroid Eros 433

6.1.1 About

Asteroid Eros 433 is a near-earth object that houses itself in the orbit between Earth and Mars. It was discovered by the German astronomer Lt. Carl Gustav Witt and French astronomer Lt. Auguste Charlois. Eros is one of the asteroids, studied and observed by the Near-Earth Asteroid Rendezvous (NEAR) [24] Shoemaker in the late 1990s with the prime objective to collect data on morphological distribution and regolith properties.

Rationale	Value
Category	Near Earth Asteroid
Mass	6.687e15 kg
Semi-major axis	1.45 au km
Sphere of Influence	350 km

Table 6.1: Specifics about Eros 433 Asteroid

6.1.2 Experimental Outcomes

The experiment was performed in an orbit, ≈ 50 km from the centre of the body. The asteroid exerts a gravitational force within a radius of sphere of influence (r_{SOI}) of ≈ 350 km . An initial path plan was developed considering the earth-based gravity measurements ¹ as shown in fig 6.1. An undulated trajectory was estimated based on the earth-based gravity model. The orbiting spacecraft approached the asteroid with the initial path plan and near-body gravitational accelerations were measured by the on-board gravimeter. This accounted for smaller gravitational accelerations acting on the body. The simulation, explored for about 1500 points, ran for 3 hours 12 minutes to reach a stable orbit, wherein the acceleration plot as in figure 6.3 seemed to remain unchanged. Also, the thrust exerted by the spacecraft showed very small changes.

The simulation provided visuals of the gradual stabilization of the orbital maneuvers. Early trajectories can be seen in fig 6.2. A visually comparative plot of the earth-based acceleration model and the in-orbit acceleration model were plotted as a digital elevation model as shown in figure 6.5 along with the trends of the decreasing thrusting exerted by the spacecraft as explorations progressed (figure 6.6).

¹Based on model available at IAU Minor Planet Center [65] and MIT Sebago [66]

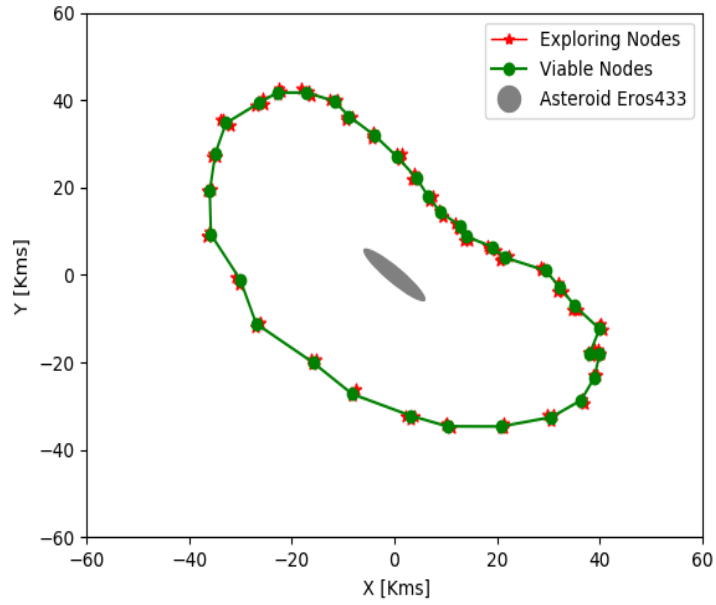


Figure 6.1: Initial path plan estimate around Eros 433 in the earth-based gravity field model

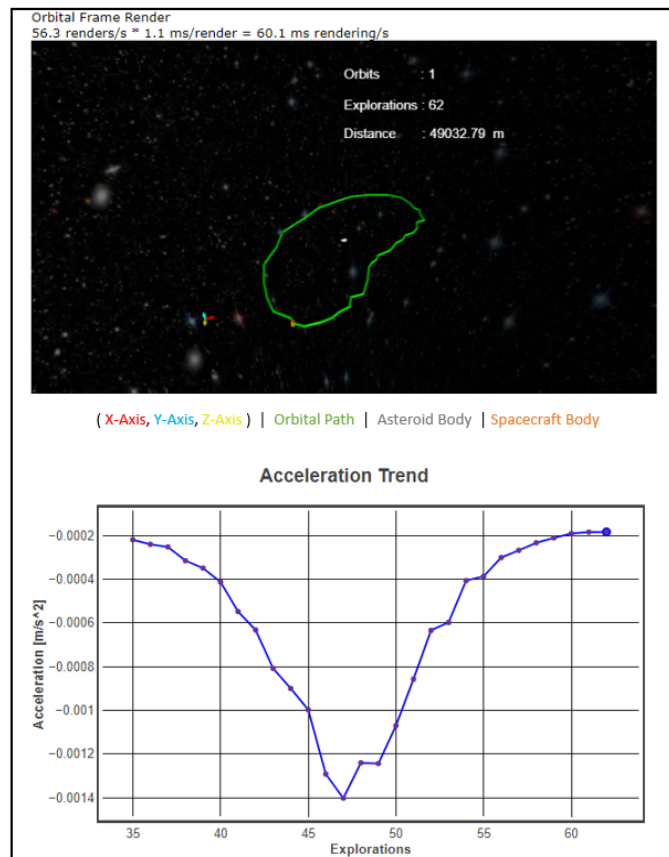


Figure 6.2: Simulation environment : exploration at a distance of 50 km from Eros 433 Asteroid

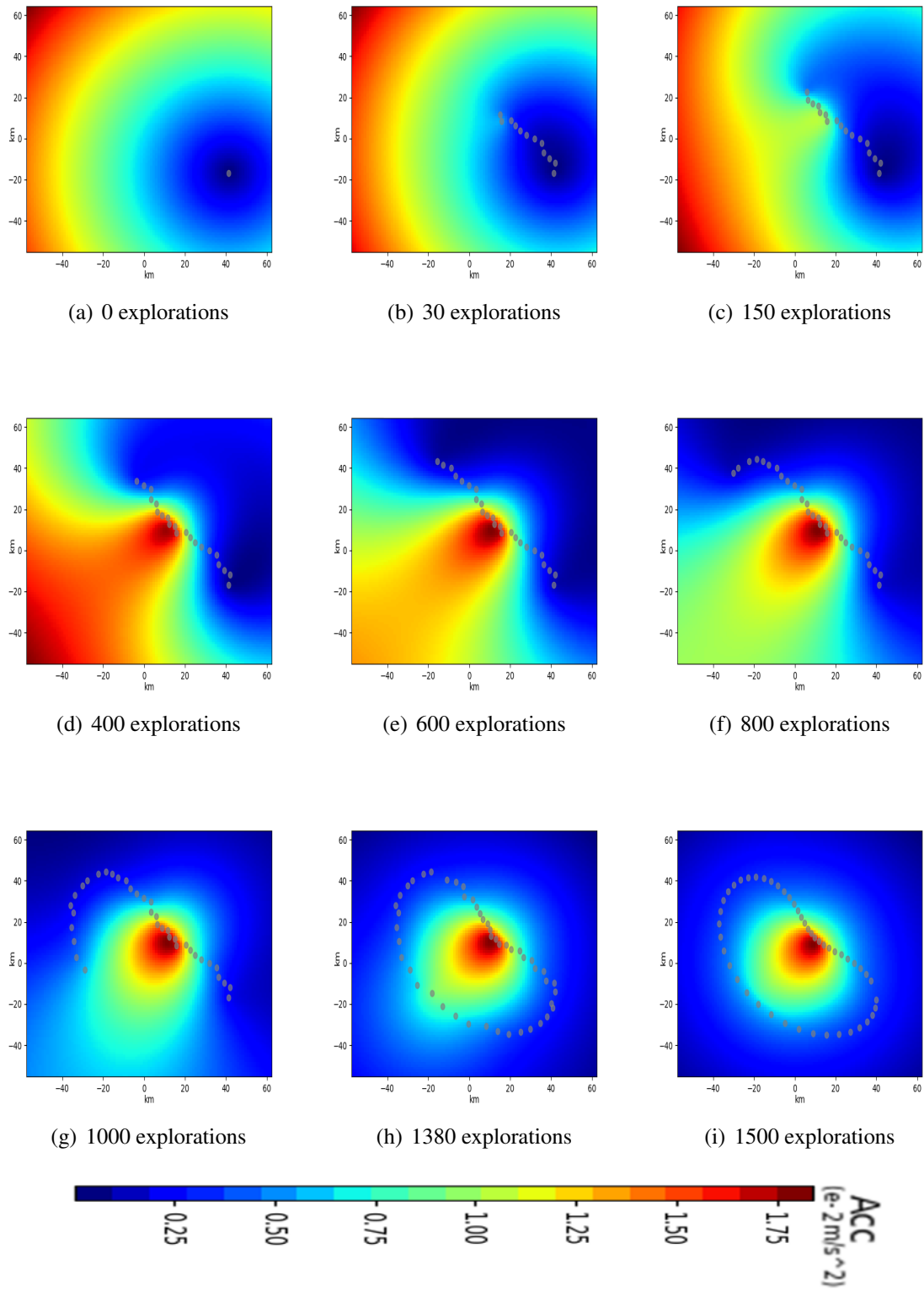
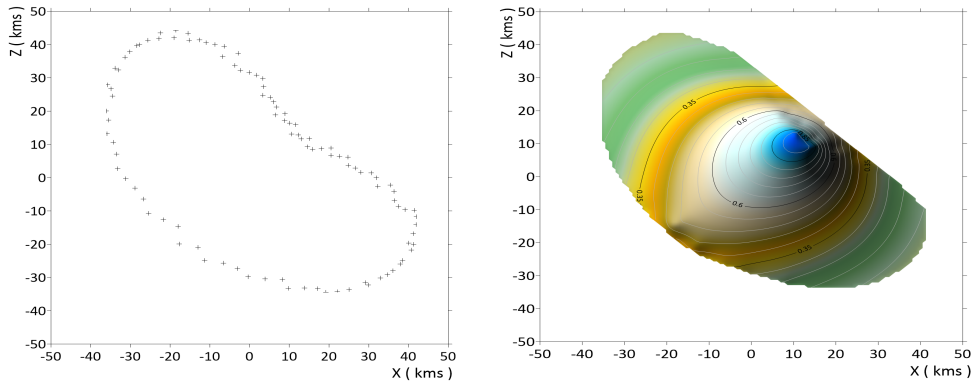
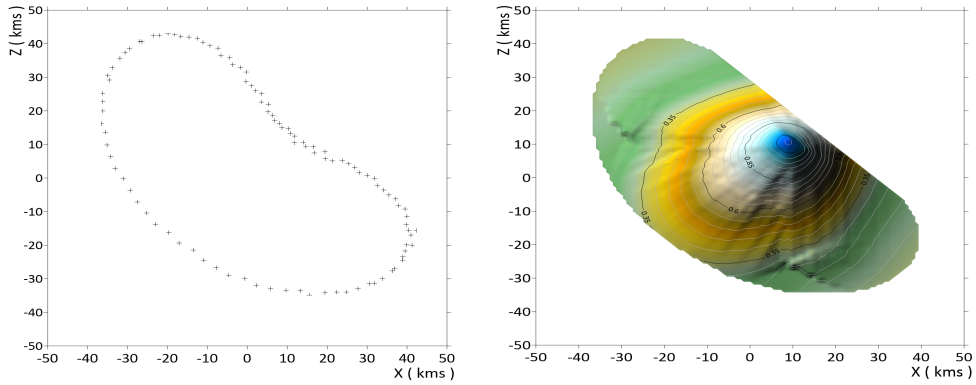


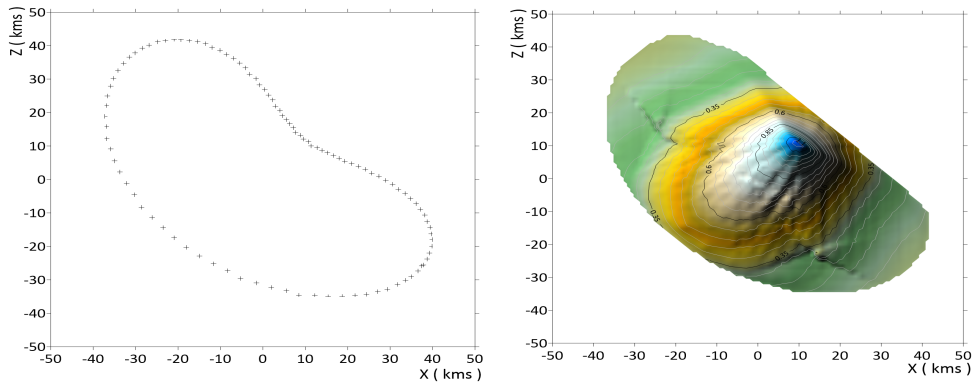
Figure 6.3: Updating Gravity field model during orbital exploration around Eros 433 asteroid



(a) Trajectory plan for 100 exploration nodes and simultaneous mapped force field



(b) Trajectory plan for 800 exploration nodes and simultaneous mapped force field



(c) Trajectory plan for 1500 exploration nodes and simultaneous mapped force field



Figure 6.4: Trajectory points for spacecraft motion at different exploration points within an orbit of 50 km from Eros 433 Asteroid with continuous updating of field model and refining orbital maneuvers

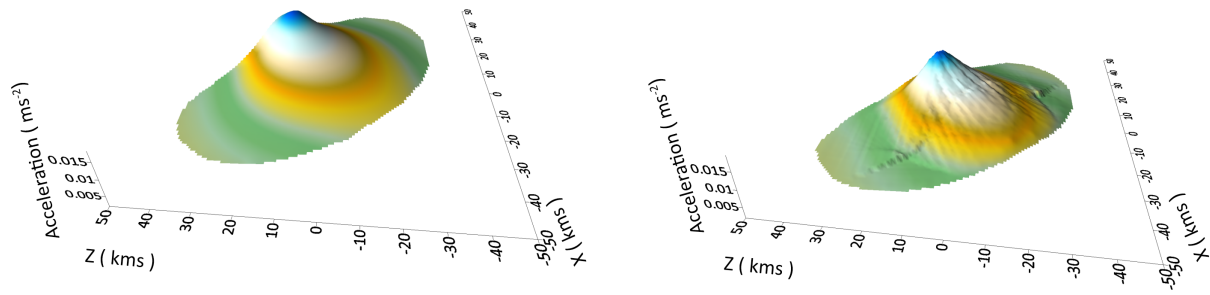


Figure 6.5: Visual Comparison of Earth-based (left) and In-Orbit (right) Gravitational Acceleration Model after 7 orbital maneuvers at a distance of 50 km

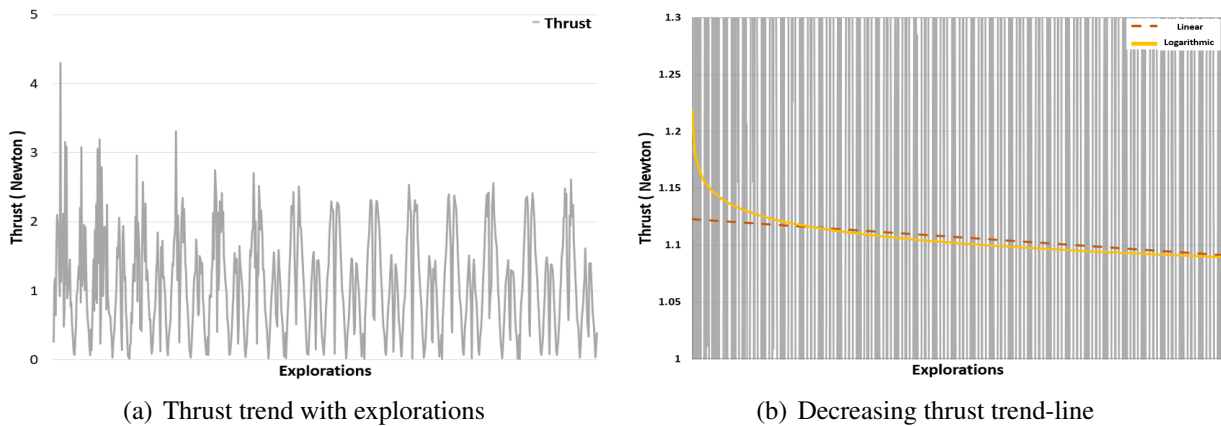


Figure 6.6: Thrust analysis for orbital motion for Asteroid Eros433

6.1.3 Result Analysis

Starting from the initial trajectory as shown in figure 6.1, the succeeding trajectories in figure 6.4 portray that the spacecraft eventually attained a stable orbit.

The updating gravity models plotted, in figure 6.3 show the constant updating of the field measurements to the on-board model. The dip in the orbit of exploration illustrates that the spacecraft experienced higher attraction and hence was pulled towards the centre of the SSSB. This required denser way-point exploration for the spacecraft to return to the safe orbit of exploration. With each maneuver as the gravity model was ‘well-informed’ of the highly attractive gravitational force in that particular space, the trajectory was corrected, eventually exploring in a smoother fashion. The values were recorded over the time span of 1500 explorations after which the spacecraft performed stable maneuvers as the field was considered to be ‘near well-known’.

A visual comparison between the earth-based measurements and the in-orbit measurements in figure 6.5 can be seen, as we achieve a higher fidelity model after the explorations, that map larger forces of attraction while accounting for the smaller forces as well. A thrust reduction of 3.06% was observed, that shows lesser thrust was exerted by the spacecraft as the maneuvers became more stable. This is synonymous to the gravity profile getting more detailed.

Locations where the gravitational pull was higher (considering the dip in the orbit), would be a favorable site study for the material composition of the asteroid and to plan landing missions.

6.2 Study 2 : Binary SSSB System

6.2.1 About

The Binary asteroid system consisting of the main body A and its moon B, were modelled within the simulation environment similar to the Didymos 65803 (which has been declared as a potential hazardous asteroid). The motion planning algorithm was tested to circumnavigate within a polar halo-orbit around the main body A, to study the potential of the receding horizon motion plan. The r_{SOI} of body A was ≈ 80 km with the gravitational field of influence of B as the tertiary (almost negligible) influential field.

Rationale	Value
Category	Near Earth Asteroid
Mass of A	1.2e14 kg
Mass of B	7.8e9 kg
Semi Major Axis of A	1.6446au km
Sphere of Influence of A	80 km

Table 6.2: Specifics about SSSB A and its moon B

6.2.2 Experimental Outcomes

The path plan as shown in figure was the initial orbital maneuver based on the earth-based gravitational field. Succeeding orbital maneuvers were based on the simultaneous measuring of the gravitational acceleration. The measured gravitational acceleration is measured by the on-board gravimeter for the spacecraft of mass 600 kg and the trends were plotted against the explored points in figure. The experiment was simulated for ≈ 5500 explored points within the orbit. The simulation run-time was logged to be 5 hours 35 minutes based on the hardware specifications mentioned in appendix 9.3.

The explored points were plotted against the measured gravitational force exerted on the spacecraft interpolated over the spatial interpolation from the spacecraft body to the surface of the asteroid. The force model was continuously updated during real time orbital maneuvers and the path was re-planned and refined considering every gravitational measurements.

Figure 6.11 shows the digital elevation model of the initial gravitational acceleration of the body based on the earth based measurements that was used to plan the initial maneuver and the model after the complete simulation as a comparison for the updated gravitational acceleration model. The trends in changing thrust were plotted as shown in figure 6.12.

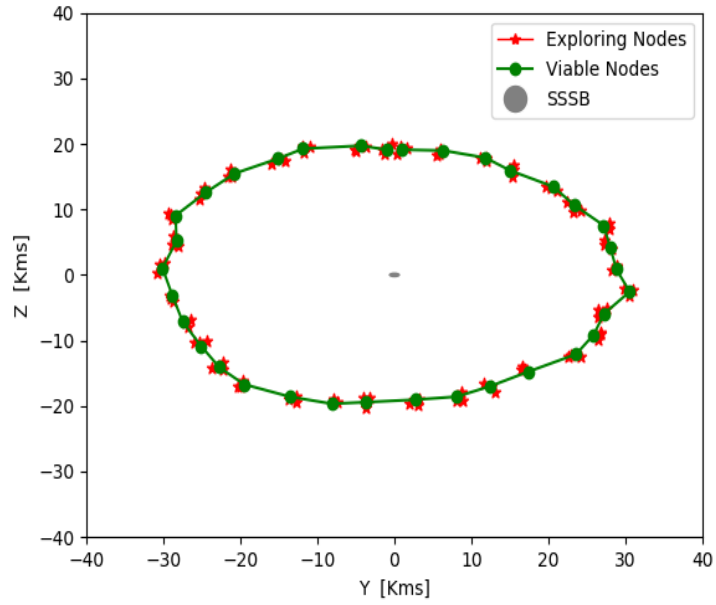


Figure 6.7: Initial path plan estimate around A in the earth-based gravity field model at a distance of 30 km (rotated 90° CW)

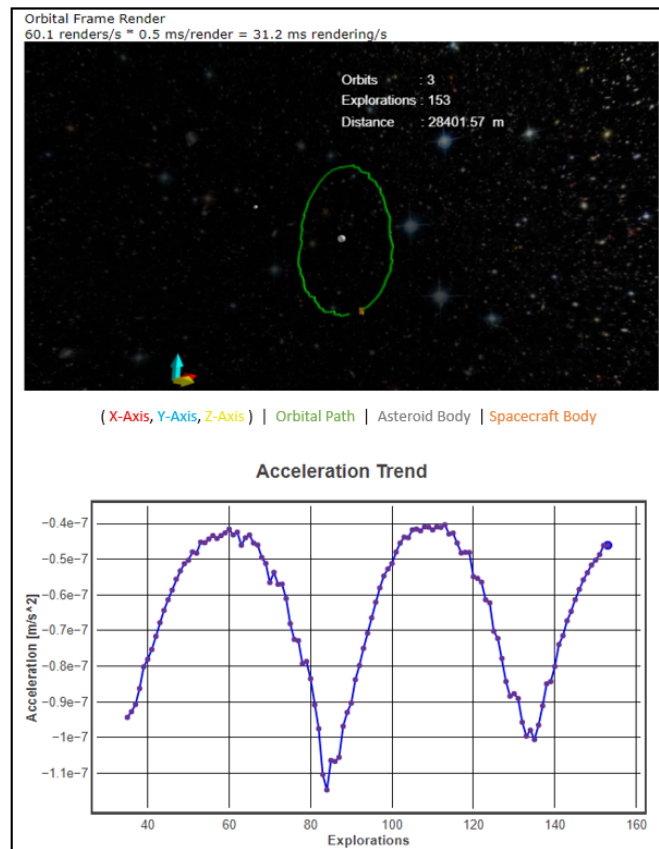


Figure 6.8: Simulation environment of exploration within halo orbit for B at a distance of 30 km from A

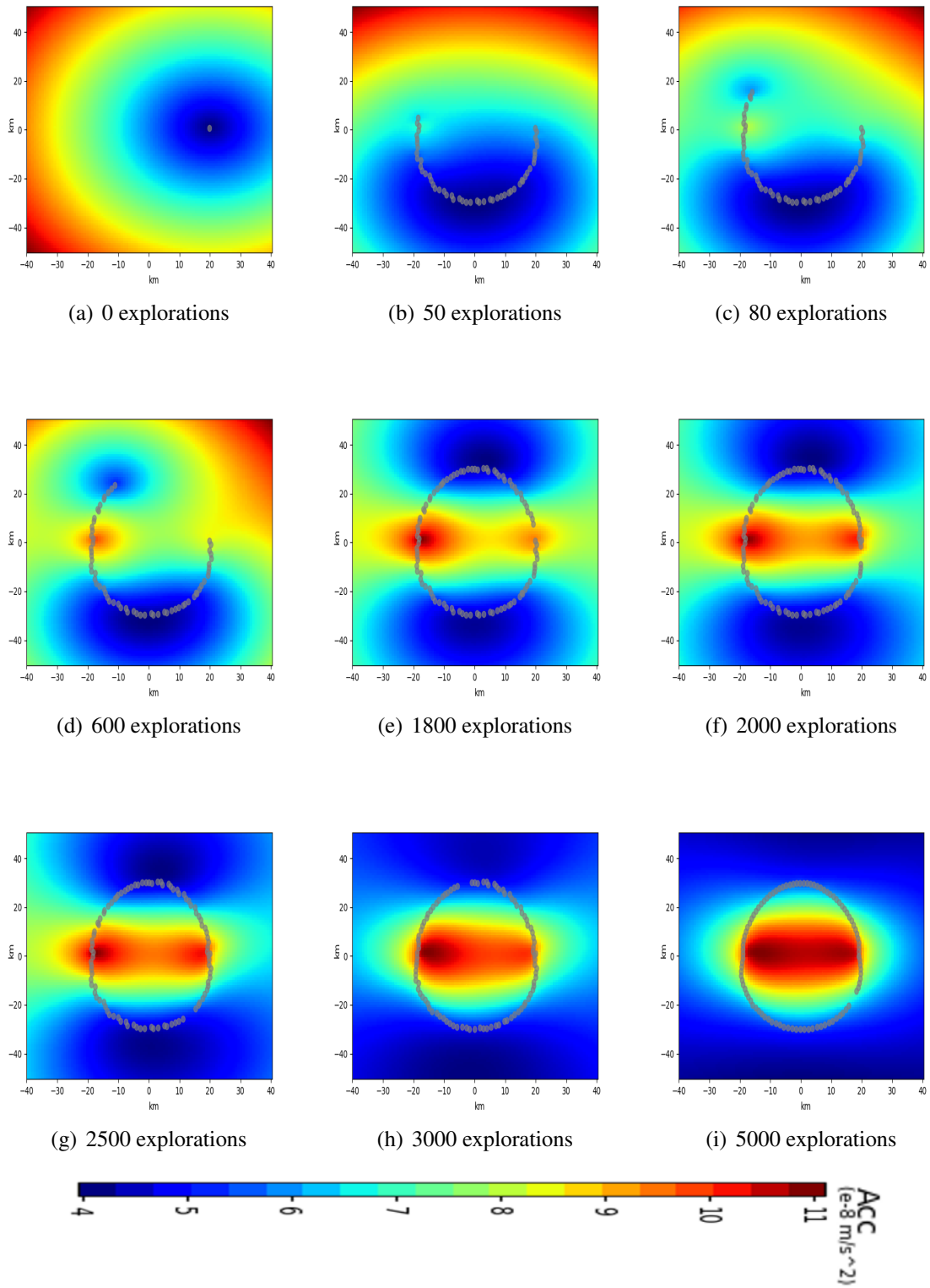
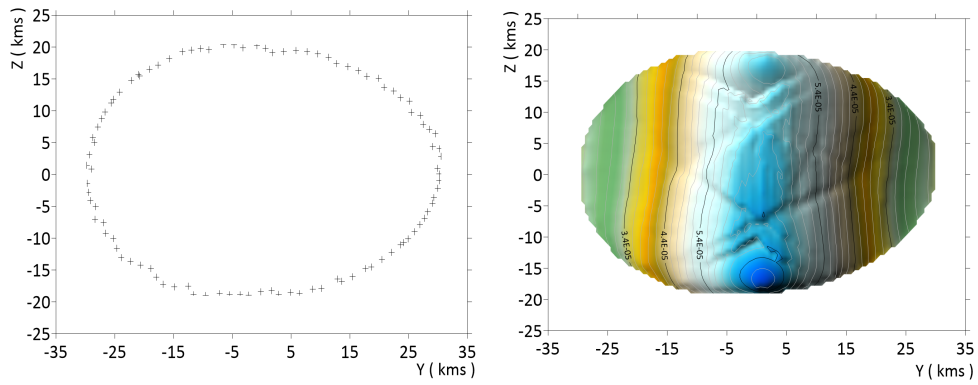
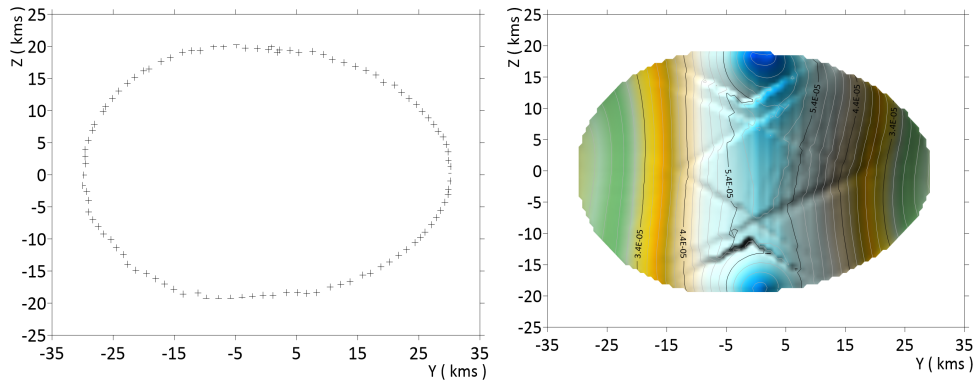


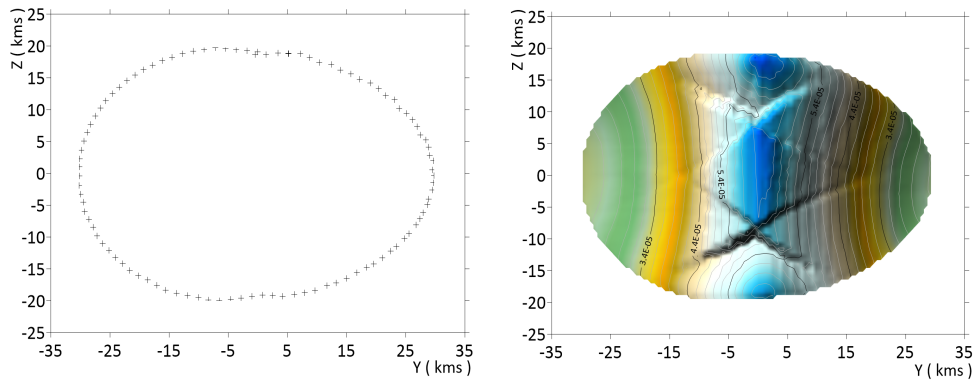
Figure 6.9: Updating Gravity field model during orbital exploration around Asteroid A



(a) Trajectory plan for 100 exploration nodes and simultaneous mapped force field



(b) Trajectory plan for 3500 exploration nodes and simultaneous mapped force field



(c) Trajectory plan for 5000 exploration nodes and simultaneous mapped force field

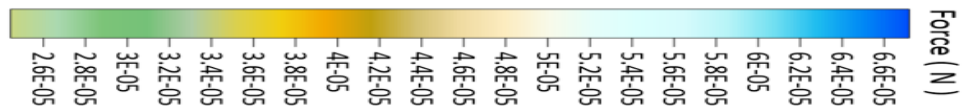


Figure 6.10: Trajectory points for spacecraft motion at different exploration points within an orbit of 30 km from SSSB A with continuous updating of field model and refining orbital maneuvers (rotated 90°CW)

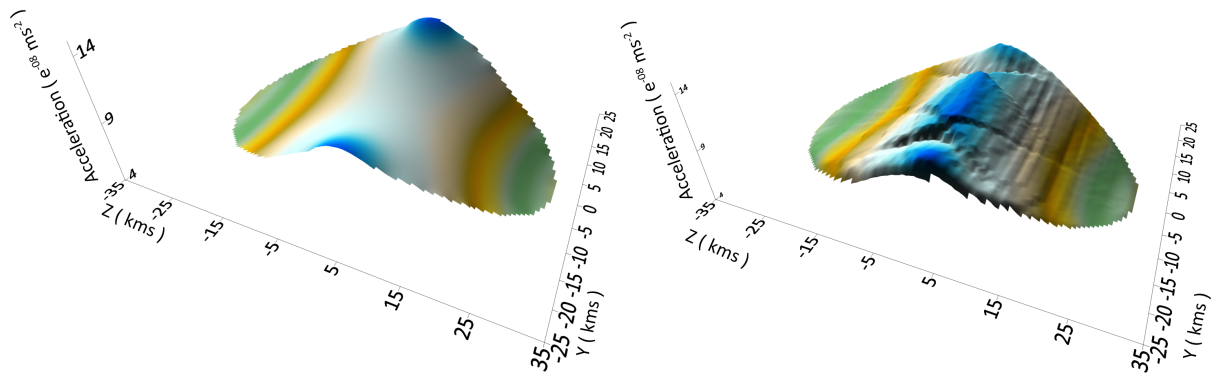


Figure 6.11: Visual Comparison of Earth-based (left) and In-Orbit (right) Gravitational Acceleration Model after 13 orbital maneuvers at a distance of 30 km

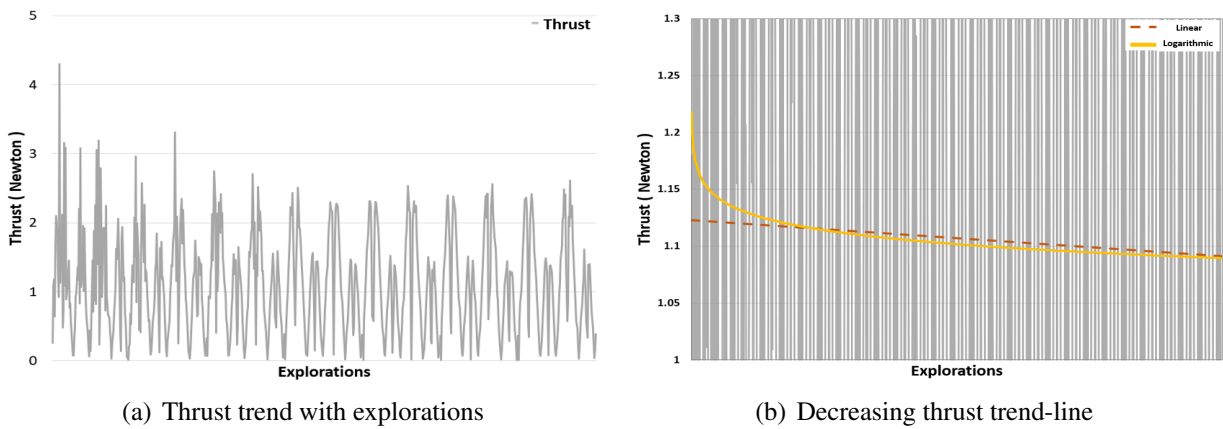


Figure 6.12: Thrust analysis for orbital motion for SSSB

6.2.3 Result Analysis

The simulation was performed in the presence of two bodies, where one orbited the other. Therefore the gravitational exertion of the moon was not prominent. The plots in figure 6.9 show that there was heavier gravitational pull at the equatorial zones of the asteroid rather than the polar zones, which also realises the orbiting of the moon in the higher gravitational influence of body A. The spacecraft however, experienced the forces at either zones and motion planning seemed to perform close to expectations wherein the smaller forces were mapped with the larger forces that can be seen with trajectories mapped in 6.10.

The smooth maneuvers indicate that the receding horizon approach was able to realise this distribution of gravity and the succeeding way-points were explored to keep the spacecraft in orbit, while simultaneously refining the maneuvers. A thrust reduction of 17.99% was observed showing that spacecraft used lesser thrusting as explorations progressed. Since the earth-based gravity model, was not well informed, it took more number of explorations for the spacecraft to realise a stable orbit in the gravitational influence of the SSSB.

The forces experienced at the equatorial zones, were close to symmetric which tell us that the body is mostly spherical. Achieving stable halo-orbits also provides the opportunity to study the moon by maintaining precise attitude control directed towards the moon.

6.3 Study 3 : Contact Binary System

6.3.1 About

A binary system field was modelled similar to that of the 486958 Arrokoth or better known as Ultima Thule (farthest visited object in the solar system by the New Horizons[13] spacecraft as a fly-by in 2019). The earth-based gravitational field was modelled to be highly attractive at the the junction of the two bodies where the acceleration is assumed to be the higher as compared to the poles of either bodies individually. The intention of the particular setup was to study the motion planning approach to consider the force of attraction at opposite ends of the body and estimate trajectories with near efficiency to stay within the orbit of exploration when intense variable forces of attraction were exerted on it.

Rationale	Value
Category	Distant Earth Object
Mass	3.12e12 kg
Semi Major Axis	44.518au km
Sphere of Influence	501.8 km

Table 6.3: Specifics about Contact binary SSSB

6.3.2 Experimental Outcomes

The simulation results revealed that the gravitational measurements were able to map the forces experienced at the poles and the contact junction. The information progressed as the spacecraft experienced the gravitational influence at the prescribed distance of exploration. The trends can be seen in figure 6.15 that show the updating knowledge of the gravitational field with subsequent maneuvers. The trajectory seemed to tend to be less chaotic in the highly variable force field, however it took many more iterations to achieve a near-stable orbit as compared to that of study 1. The simulation run-time was logged to be 7 hours 10 minutes to compute a trajectory that was refined with explorations.

The trajectories, explored for about 7000 points, can be seen to smoothen as plotted in figure 6.16 along with the gravitational forces that were mapped and interpolated over the spatial interpolation up-to the centre of the SSSB and a higher fidelity gravitational acceleration model was obtained as can be compared in figure 6.17.

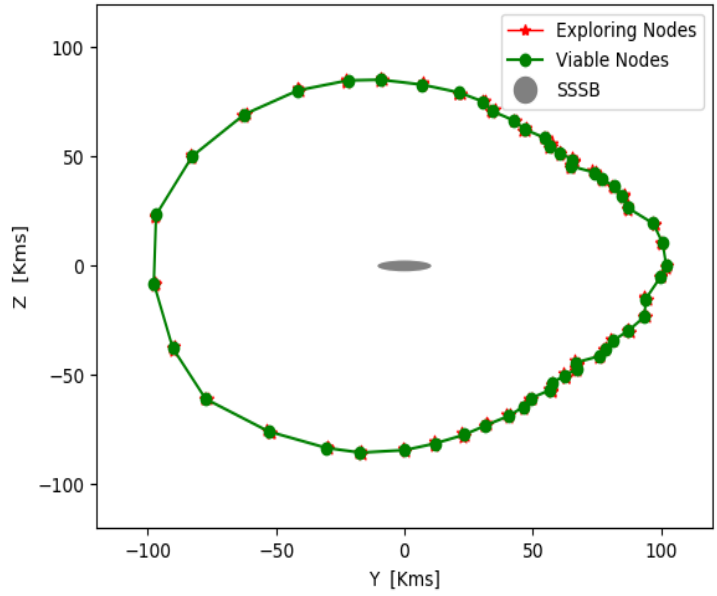


Figure 6.13: Initial path plan estimate around SSSB in the earth-based gravity field model at a distance of 100 km

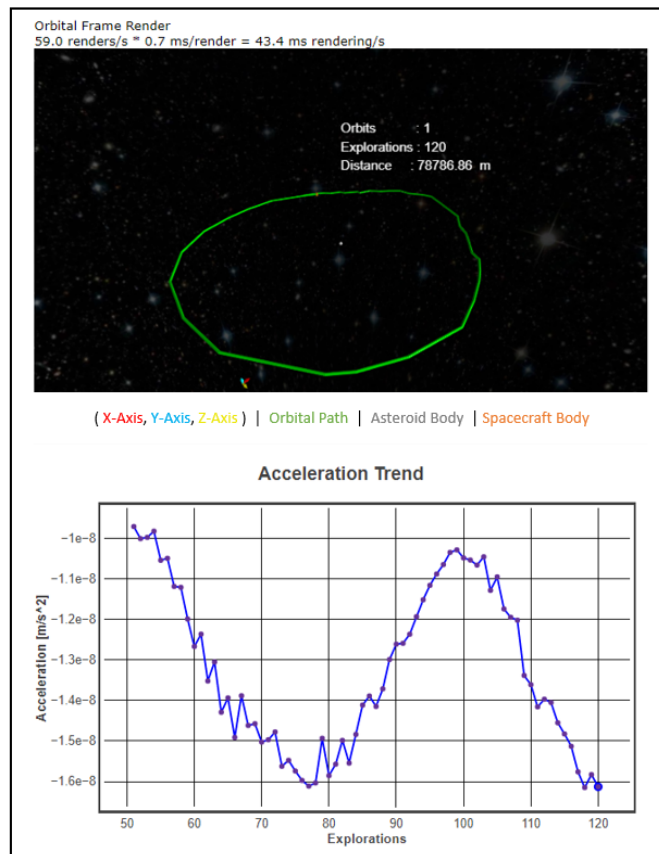


Figure 6.14: Simulation environment of exploration at a distance of 100 km

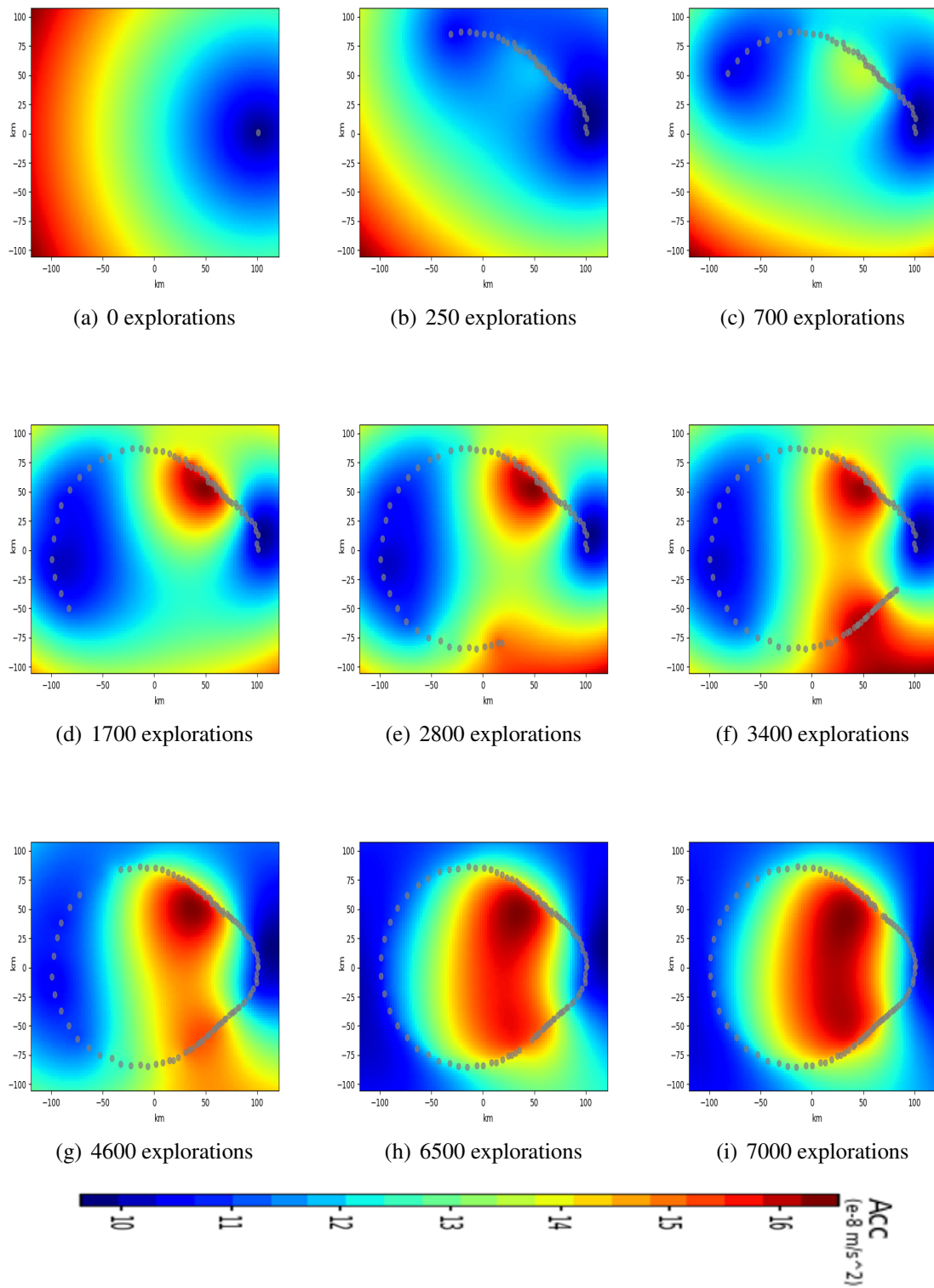
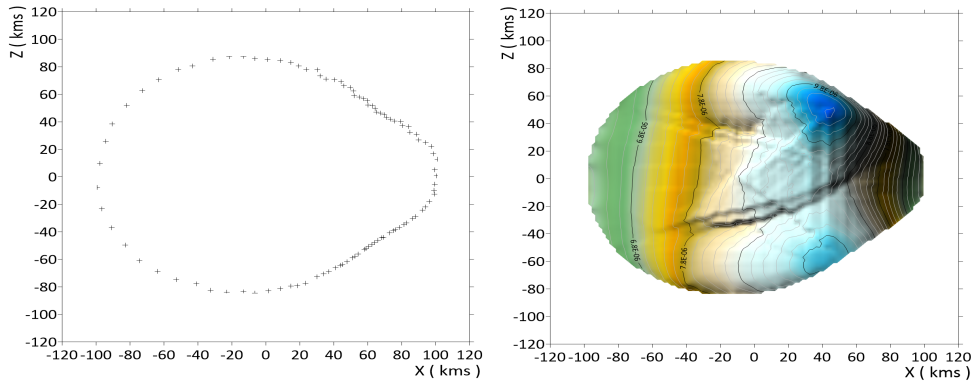
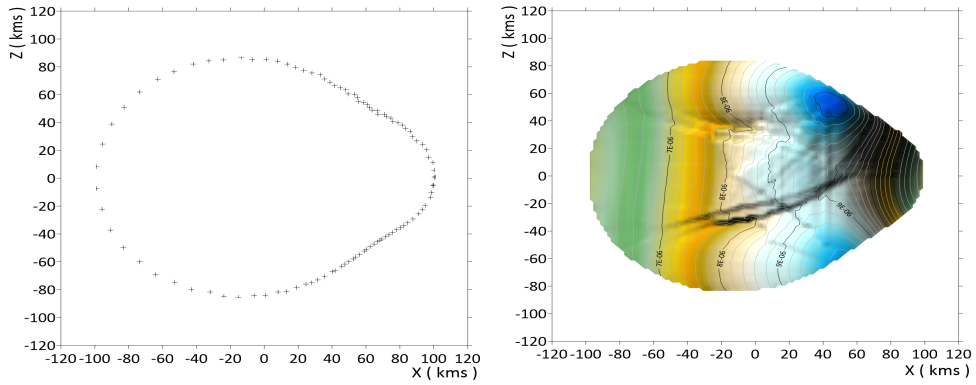


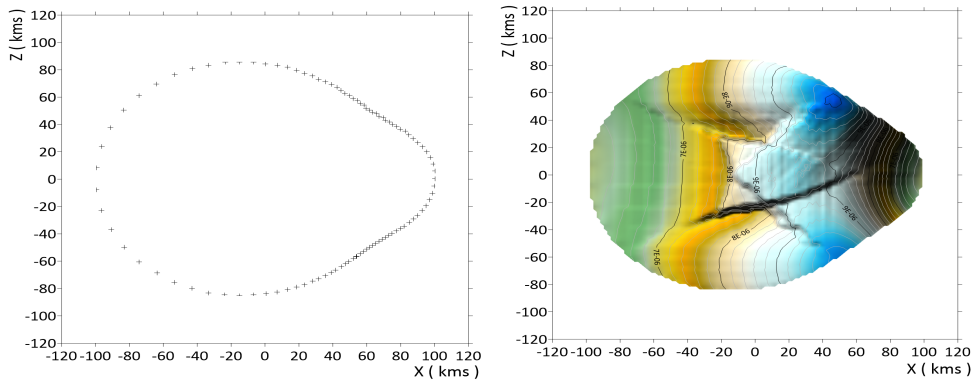
Figure 6.15: Updating Gravity field model during orbital exploration around SSSB



(a) Trajectory plan for 100 exploration nodes and simultaneous mapped force field



(b) Trajectory plan for 3000 exploration nodes and simultaneous mapped force field



(c) Trajectory plan for 7000 exploration nodes and simultaneous mapped force field

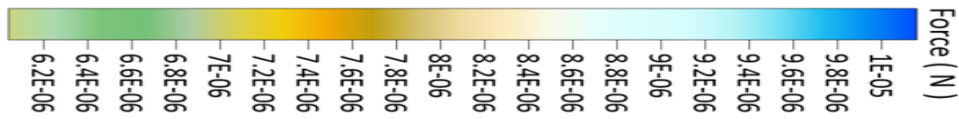


Figure 6.16: Trajectory points for spacecraft motion at different exploration points within an orbit of 100 km from SSSB with continuous updating of field model and refining orbital maneuvers

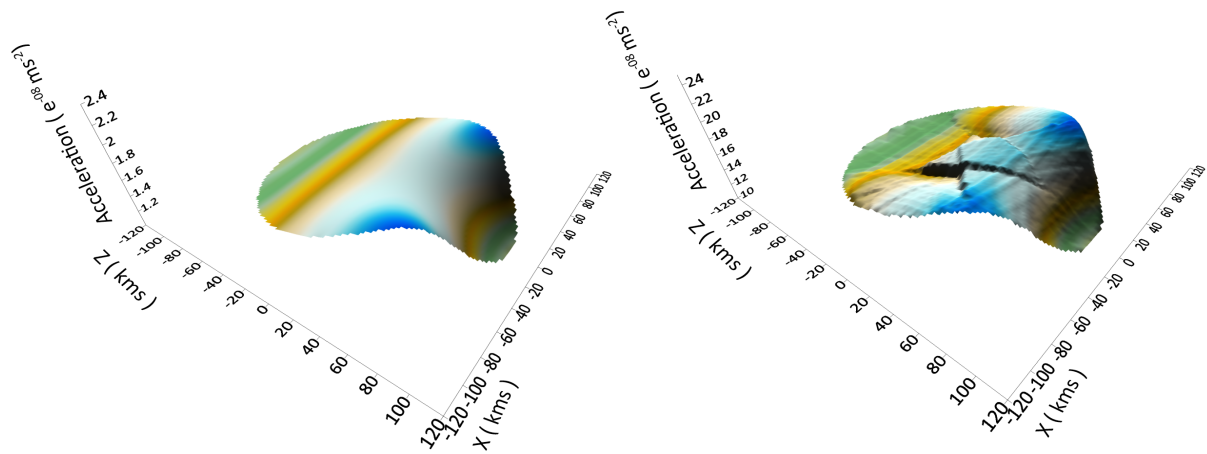


Figure 6.17: Visual Comparison of Earth-based (left) and In-Orbit (right) Gravitational Acceleration Model after 19 orbital maneuvers at 100 km

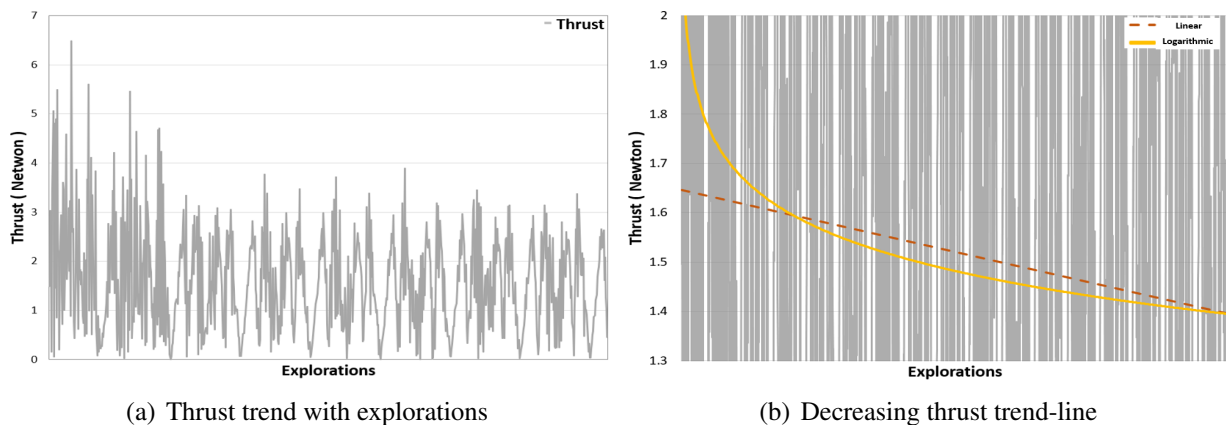


Figure 6.18: Thrust analysis for orbital motion for SSSB

6.3.3 Result Analysis

The results show that the motion planning approach was able to explore in the gravity field. The measurements were able to map the irregularity and prescribe trajectories accordingly to stay within orbit of exploration.

The gravitational model provides the information of higher gravitational acceleration at the junction which is where the two bodies are co-joined, thus conveying the approximated location of the junction. As the model was more erratic, the receding horizon simulated the trajectories for a higher number of iterations in order to realize stable orbital maneuvers. The acceleration plots in figure 6.17 illustrate that there were more forces to be considered as compared to those obtained from the earth-based observations and measurements. A thrust reduction of 24.29% was noted to show the decrease in spacecraft thrust as the motion became stable.

The research defines the premise of not only mapping the gravitational field of the bodies, but also conveying relevant information about their anatomy. This can help plan future missions as flyby or even landing with additional instruments that base their trajectories on the high fidelity model obtained by the active maneuvering in the vicinity of the SSSB.

7 Further Contributions

The following research has the potential to contribute to various missions and applications that could further the use-case of dynamic path planning. A few application areas have been discussed below.

- **Upcoming Missions**

- Double Asteroid Redirection Test (DART, 2021 [67])

The DART mission intends to impact Didymoon with a kinetic impactor and study the events that follow. The impacting spacecraft could make use of optimal path planning supporting the on-board SmartNav system and with updated knowledge of the gravitational field sight trajectories and soft spots on the surface to impact the asteroid's moon.

- Multi Asteroid Touring (MAT [68])

The research can be furthered for the Multi-Asteroid Touring concept to explore multiple asteroids within the asteroid belt in a single mission. The fleet of satellites could operate over a swarm-based topology with active re-planning to study multiple asteroids.

- **Mapping of Dynamic Processes**

All processes in nature are dynamic and understanding their intricacies requires measurements at multiple locations and different time instances. Examples of dynamic events are jets from comets and debris plumes formed during impacts, or terrestrial cases like forest fires, erupting geysers and explosive mining. These dynamic processes could be mapped with optimal path planning approaches. The path plans could estimate viable points where the vehicles could be present at anticipated times, to map certain events.

- **Aiding Scientific Experiments**

Scientific experiments like measuring albedo and topographical mapping could be performed at designated points during active re-planning to scout specific areas.

- **On-Board Resource Utilisation**

Optimal path planning and deeper knowledge of the gravitational distribution can contribute to efficient on-board resource utilisation like fuel consumption for propulsion to thrust at certain points during exploration.

8 Conclusion

A novel motion planning approach was demonstrated to realise dynamic and autonomous orbital exploration around small solar system bodies using the arbitrary gravitational forces exerted by the body. The experimental outcomes discussed in this thesis, showcase the feasibility of the motion planning algorithm as an efficient approach to execute safe maneuvers in the gravitational field and obtain fine-grained field models. The stable orbital trajectory achieved within the sphere of influence proves the competence of using a receding horizon approach.

It can be concluded that Earth-based observations are adequate to reach the SSSB but not 'well-informed' enough to perform orbital maneuvers in the vicinity of SSSB to study them better, which is where dynamic path planning plays a crucial role.

The project can be progressed by considering multiple orbits of exploration by a single spacecraft to map the gravitational field from different stable orbits. The dynamic motion planning algorithm can also be modelled for a swarm-based spacecraft system to explore optimal points within the orbit as plan for experiments as mentioned in chapter 7. Terrestrial applications for the same can be developed to study dynamic events.

Considering the aforementioned, the research motivates possible collaboration of the robotics and space community to work collectively by sharing the respective domain knowledge towards space robotics. This merger promises to advance robot-assisted activities and unmanned explorations to places that are beyond the reach of humans, yet.

Eventually, such endeavors stimulate our curiosity to gain knowledge of what lies beyond the realms of the Earth with the ambition to be able to truly 'Define Our Space'.

Acknowledgements

I feel privileged to have been guided and mentored by my very able supervisors **Dr. Michael W. Otte** and **Mr. Viljo Allik**. Their constant guidance, throughout the tenure has been prime in completion of the work. From technical suggestions to full-filing bureaucratic proceedings and battling the lock-down (due to the pandemic outrage of the corona virus), their support was not only motivating but also warming enough for me to continuously believe in the research and progress with it every single day.

My heartfelt gratitude to the **University of Tartu**, and **Tartu Observatory** for providing me with the research-oriented environment and infrastructure that made the thesis a possibility.

My aspirations were nurtured by my grandparents and parents, to whom I extend my appreciation and regards for having inspired me and continue to do so. A special mention to friends and colleagues who filled this journey with critical insights, new learning, fun and laughter.

This research work explored new disciplines of space and robotics engineering. Pursuing this research has developed in me, profound respect for scientists and engineers who dedicate their time and energy to research and develop novel techniques in exploring new realms of knowledge.

Abhitya Sawio Paul

Bibliography

- [1] “common elementary research classification scheme (cercs)”. [online] URL : <https://www.etis.ee/Portal/Classifiers/Details/d3717f7b-bec8-4cd9-8ea4-c89cd56ca46e>, [Accessed : 03.03.2020].
- [2] ”JPL small body database browser” [online] URL : <https://ssd.jpl.nasa.gov/sbdb.cgi?sstr=1orb=1top>[accessed = 01.15.2020].
- [3] “small bodies of the solar system”. [online] URL : <https://science.nasa.gov/solar-system/focus-areas/small-bodies-solar-system> [Accessed : 08.15.2019], .
- [4] ”international astronomical congress”. [online] URL : <https://www.iau.org/>[Accessed : 09.23.2020].
- [5] Francesca DeMeo, Conel Alexander, Kevin Walsh, Clark Chapman, and Richard Binzel. The compositional structure of the asteroid belt. *Asteroids IV*, 06 2015. doi: 10.2458/azu_uapress_9780816532131-ch002. URL <https://arxiv.org/abs/1506.04805>.
- [6] Brett Gladman, J.J. Kavelaars, J.-M Petit, Alessandro Morbidelli, Matthew Holman, and Thomas Lored. The structure of the kuiper belt: Size distribution and radial extent. *The Astronomical Journal*, 122:1051, 12 2007. doi: 10.1086/322080. URL <https://iopscience.iop.org/article/10.1086/322080/meta>.
- [7] ”small solar system bodies at estec”. [online] URL : <https://www.cosmos.esa.int/web/estec-science-faculty/small-solar-system-bodies>[Accessed : 09.23.2020], .
- [8] ”asteroids:european space agency”. [online] URL : https://www.esa.int/Science_Exploration/Human_and_Robotic_Exploration/Exploration/Asteroids[Accessed : 09.23.2020].
- [9] Deborah Domingue and Andrew Cheng. Near earth asteroid rendezvous: the science of discovery. *Johns Hopkins APL Technical Digest*, 23, 01 2002. URL https://www.researchgate.net/publication/252558335_Near_Earth_Asteroid_Rendezvous_the_science_of_discovery.
- [10] M. Combi, Maria Capria, Gabriele Cremonese, Maria Cristina De Sanctis, Tony Farnham, Y. Fernandez, M. Festou, U. Fink, Jacklyn Green, Walter Harris, Carl Hergenrother, Philippe Lamy, Stephen Larson, H. Levison, D. Lien, Carey Lisse, D. Meisel, D. Möhlmann, Beatrice Mueller, and Paul Weissman. The study of comets. 272: 323–336, 07 2002. URL https://www.researchgate.net/publication/234390665_The_Study_of_Cometes.

- [11] "Soho's new catch". [online] URL : http://www.esa.int/Science_Exploration/Space_Science/SOHO_s_new_catch_its_first_officially_periodic_comet [Accessed : 09.25.2020].
- [12] "what are planetoids?" URL : <https://www.universetoday.com/37116/planetoid/amp/> [accessed : 03.05.2020].
- [13] "nasa resources : Solar system exploration - comets". [online] URL : https://www.nasa.gov/mission_pages/newhorizons/main/index.html [Accessed : 09.17.2020].
- [14] "nasa resources : Solar system exploration - asteroids" [online] URL : https://solarsystem.nasa.gov/resources/780/nears-first-whole-eros-mosaic-from-orbit/?category=planets_jupiter [Accessed : 09.17.2020], .
- [15] "nasa resources : Solar system exploration - comets" [online] URL : https://solarsystem.nasa.gov/resources/510/rosettacometfrom177miles/?category=small-bodies_comets [Accessed : 09.17.2020].
- [16] "ultima thule : Planetoid" URL : <https://www.nasa.gov/feature/aprehistoricpuzzleinthe-kuiperbelt> [Accessed : 01.10.2020].
- [17] Oyvind Gron. Newton's law of universal gravitation. *Lecture Notes in Physics*, 02 2009. doi: 10.1007/978-0-387-88134-8_1. URL https://link.springer.com/chapter/10.1007%2F978-0-387-88134-8_1.
- [18] B. Tapley, Srinivas Bettadpur, Michael Watkins, and Christoph Reigber. The gravity recovery and climate experiment: Mission overview and early results. *Geophysical Research Letters*, 31:4 PP., 05 2004. doi: 10.1029/2004GL019920. URL <https://agupubs.onlinelibrary.wiley.com/doi/abs/10.1029/2004GL019920>.
- [19] "GRACE: JGM global gravity model". [online] URL : <https://photojournal.jpl.nasa.gov/catalog/PIA12146> [Accessed : 10.10.2020], .
- [20] "the nasa gsfc and nima joint geopotential model". [online] URL : <https://cddis.nasa.gov/926/egm96/egm96.html> [Accessed : 10.10.2020], .
- [21] D Hyland, H. Altwaijry, Hong Sup Kim, Neha Satak, and S Ge. Nea mitigation via the yarkovsky effect. volume 150, 01 2013. URL https://www.researchgate.net/publication/269929507_NEA_mitigation_via_the_Yarkovsky_effect.
- [22] Alessio Vigna, Laura Faggioli, A. Milani, Federica Spoto, Davide Farnocchia, and Benoit Carry. Detecting the yarkovsky effect among near-earth asteroids from astrometric data, 05 2018. URL <https://arxiv.org/abs/1805.05947v1>.
- [23] "ICGEM gravity models" [online] URL : http://icgem.gfz-potsdam.de/tom_longtime [[Accessed : 01.12.2020]].
- [24] A.G. Santo, S.C. Lee, and Andrew Cheng. Near earth asteroid rendezvous spacecraft overview. pages 131 – 144 vol.2, 03 1996. ISBN 0-7803-3196-6. doi: 10.1109/AERO.1996.495972. URL https://www.researchgate.net/publication/3626764_Near_Earth_asteroid_rendezvous_spacecraft_overview.

- [25] Andrew Cheng. Near earth asteroid rendezvous: Mission summary. *Asteroids III*, 01 2002. URL <https://history.nasa.gov/monograph36.pdf>.
- [26] "near collected shape and gravity models" [online] URL : <https://sbn.psi.edu/pds/resource/nearbrowse.html> [Accessed : 09.21.2020].
- [27] "astrodynamics and the gravity measurement descent operation". [online] URL : http://www.hayabusa2.jaxa.jp/en/topics/20181225e_AstroDynamics/ [accessed : 12.25.2019].
- [28] Kieran Carroll and Daniel Faber. Tidal acceleration gravity gradiometry for measuring asteroid gravity field from orbit. 10 2018. URL https://www.researchgate.net/publication/328828084_Tidal_Acceleration_Gravity_Gradiometry_for_Measuring_Asteroid_Gravity_Field_From_Orbit.
- [29] L. E. Kavraki, P. Svestka, J. . Latombe, and M. H. Overmars. Probabilistic roadmaps for path planning in high-dimensional configuration spaces. *IEEE Transactions on Robotics and Automation*, 12(4):566–580, Aug 1996. ISSN 2374-958X. doi: 10.1109/70.508439. URL https://www.cs.cmu.edu/~motionplanning/papers/sbp_papers/PRM/prmbasic_01.pdf.
- [30] Steven M. Lavalle. Rapidly-exploring random trees a new tool for path planning. Technical report, 1998. URL <http://msl.cs.illinois.edu/~lavalley/papers/Lav98c.pdf>.
- [31] Steven M. LaValle and Jr. James J. Kuffner. Randomized kinodynamic planning. *The International Journal of Robotics Research*, 20(5):378–400, 2001. doi: 10.1177/02783640122067453. URL <https://doi.org/10.1177/02783640122067453>.
- [32] Z. Littlefield, Y. Li, and K. E. Bekris. Efficient sampling-based motion planning with asymptotic near-optimality guarantees for systems with dynamics. In *IEEE/RSJ International Conference on Intelligent Robots and Systems (IROS)*, Tokyo Big Sight, Japan, 11/2013 2013. URL http://www.cs.rutgers.edu/~kb572/pubs/sparse_rrt_iros13.pdf.
- [33] Sertac Karaman and Emilio Frazzoli. Sampling-based algorithms for optimal motion planning. *The international journal of robotics research*, 30(7):846–894, 2011. doi: 10.1177/0278364911406761. URL <https://journals.sagepub.com/doi/10.1177/0278364911406761>.
- [34] Kouros Naderi, Joose Rajamäki, and Perttu Hämmäläinen. Rt-rrt*: a real-time path planning algorithm based on rrt*. pages 113–118, 11 2015. doi: 10.1145/2822013.2822036. URL <https://dl.acm.org/doi/10.1145/2822013.2822036>.
- [35] Michael Otte and Emilio Frazzoli. RRTX: Asymptotically optimal single-query sampling-based motion planning with quick replanning. *The International Journal of Robotics Research*, 35(7):797–822, 2016. doi: 10.1177/0278364915594679. URL <http://ijr.sagepub.com/cgi/content/abstract/35/7/797>.
- [36] Yanbo Li, Zakary Littlefield, and Kostas E. Bekris. Asymptotically optimal sampling-based kinodynamic planning. *The International Journal of Robotics Research*, 35(5):

- 528–564, 2016. doi: 10.1177/0278364915614386. URL <https://doi.org/10.1177/0278364915614386>.
- [37] Panagiotis Tsiotras. On-line path generation and tracking for high-speed wheeled autonomous vehicles. 02 2006. URL <https://apps.dtic.mil/dtic/tr/fulltext/u2/a447359.pdf>.
- [38] Karl Worthmann. *Stability Analysis of Unconstrained Receding Horizon Control Schemes*. PhD thesis, 01 2011. URL <https://www.semanticscholar.org/paper/Stability-Analysis-of-Unconstrained-Receding-Worthmann/12b20a4a2d3436b669564bc9612842fc41468d13>.
- [39] C. J. Golden. The why and how of satellite autonomy. In *MILCOM 88, 21st Century Military Communications - What's Possible?*. Conference record. Military Communications Conference, pages 853–857 vol.3, Oct 1988. doi: 10.1109/MILCOM.1988.13490. URL <https://ieeexplore.ieee.org/document/13490>.
- [40] Arthur Richards, Tom Schouwenaars, Jonathan P How, and Eric Feron. Spacecraft trajectory planning with avoidance constraints using mixed-integer linear programming. *Journal of Guidance, Control, and Dynamics*, 25(4):755–764, 2002. doi: 10.2514/2.4943. URL <http://www.et.byu.edu/~beard/papers/library/RichardsEtAl02.pdf>.
- [41] Dario Izzo and Lorenzo Pettazzi. Autonomous and distributed motion planning for satellite swarm. *Journal of Guidance, Control, and Dynamics*, 30(2):449–459, 2007. doi: 10.2514/1.22736. URL <https://arc.aiaa.org/doi/10.2514/1.22736>.
- [42] David P Dannemiller. Multi-maneuver clohessy-wiltshire targeting. 2011. URL <https://ntrs.nasa.gov/search.jsp?R=20110008472>.
- [43] Hari B Hablani, Myron L Tapper, and David J Dana-Bashian. Guidance and relative navigation for autonomous rendezvous in a circular orbit. *Journal of guidance, control, and dynamics*, 25(3):553–562, 2002. doi: 10.2514/2.4916. URL <https://arc.aiaa.org/doi/abs/10.2514/2.4916?journalCode=jgcd>.
- [44] Ismael Lopez and Colin R McInnes. Autonomous rendezvous using artificial potential function guidance. *Journal of Guidance, Control, and Dynamics*, 18(2):237–241, 1995. doi: 10.2514/3.21375. URL <https://arc.aiaa.org/doi/10.2514/3.21375>.
- [45] "algorithmic foundations for realtime and dependable spacecraft motion planning". [online] URL : https://www.nasa.gov/pdf/678821main_pavone_summary.pdf [Accessed : 12.13.2020].
- [46] Zachary Kingston, Mark Moll, and Lydia E. Kavraki. Sampling-based methods for motion planning with constraints. *Annual Review of Control, Robotics, and Autonomous Systems*, 1(1):159–185, 2018. doi: 10.1146/annurev-control-060117-105226. URL <https://doi.org/10.1146/annurev-control-060117-105226>.
- [47] "newton's law of gravitation" URL : <https://www.britannica.com/science/Newtons-law-of-gravitation> [accessed : 05.10.2020].

- [48] Douglas Macdougall. *Newton's Gravity*. 01 2012. doi: 10.1007/978-1-4614-5444-1. URL <https://www.springer.com/gp/book/9781461454434>.
- [49] Alex Soumbatov-Gur. Predictions for osiris-rex mission at asteroid bennu, 11 2018. URL https://www.researchgate.net/publication/328852093_Predictions_for_OSIRIS-REx_mission_at_asteroid_Bennu?channel=doi&linkId=5be667b24585150b2bab8a7b&showFulltext=true.
- [50] "DARPA robotics challenge". [online] URL : <https://www.darpa.mil/> [Accessed : 02.12.2020].
- [51] Atsushi Sakai, Daniel Ingram, Joseph Dinius, Karan Chawla, Antonin Raffin, and Alexis Paques. Pythonrobotics: a python code collection of robotics algorithms. *CoRR*, abs/1808.10703, 2018. URL <http://arxiv.org/abs/1808.10703>.
- [52] Brian Paden, Michal Čáp, Sze Zheng Yong, Dmitry Yershov, and Emilio Frazzoli. A survey of motion planning and control techniques for self-driving urban vehicles. *IEEE Transactions on intelligent vehicles*, 1(1):33–55, 2016. doi: 1604.07446. URL <https://arxiv.org/abs/1604.07446>.
- [53] David González, Joshué Pérez, Vicente Milanés, and Fawzi Nashashibi. A review of motion planning techniques for automated vehicles. *IEEE Transactions on Intelligent Transportation Systems*, 17(4):1135–1145, 2015. doi: 10.1109/TITS.2015.2498841. URL <https://ieeexplore.ieee.org/document/7339478>.
- [54] Josie Hughes, Masaru Shimizu, and Arnoud Visser. A review of robot rescue simulation platforms for robotics education. In *Robot World Cup*, pages 86–98. Springer, 2019. doi: 10.1007/978-3-030-35699-6_7. URL https://link.springer.com/chapter/10.1007%2F978-3-030-35699-6_7.
- [55] Steven Hughes, Darrel Conway, and Joel Parker. Using the general mission analysis tool (gmat), 02 2017. URL https://www.researchgate.net/publication/313994327_Using_the_General_Mission_Analysis_Tool_GMAT?channel=doi&linkId=58b0fcda92851cf7ae8bbf35&showFulltext=true.
- [56] Steve Parkes, I. Martin, M. Dunstan, and D. Matthews. Planet surface simulation with pangu. 05 2004. doi: 10.2514/6.2004-592-389. URL <https://arc.aiaa.org/doi/10.2514/6.2004-592-389>.
- [57] J. Binder. Planning space missions with freeflyer. 43:24–25, 07 2005. URL https://www.researchgate.net/publication/296901038_Planning_space_missions_with_FreeFlyer.
- [58] Luc Maisonobe, Véronique Pommier, and Pascal Parraud. Orekit: An open source library for operational flight dynamics applications. 04 2010. URL <https://www.researchgate.net/project/Orekit>.
- [59] Dr Annadurai, Dr TK, Rama Murali G K, and Krishnan A. Chandrayaan-1 mission challenges and unique features. 11 2012. URL https://www.researchgate.net/publication/282752531_Chandrayaan-1_Mission_Challenges_and_Unique_Features.

- [60] Kravaris C. Berber R. Non linear model predictive control schemes with guaranteed stability. *NATO ASI Series: Applied Science*, 353, 1998. doi: 10.1007/978-94-011-5094-1_16. URL https://doi.org/10.1007/978-94-011-5094-1_16.
- [61] "receding horizon trajectory optimization with terminal impact". [online] URL : https://www.researchgate.net/publication/268387226_Receding_Horizon_Trajectory_Optimization_with_Terminal_Impact_Specifications/figures?lo=1 [Accessed : 12.23.2020].
- [62] Meng Wang, Martin Treiber, Winnie Daamen, Serge Hoogendoorn, and B. Arem. Modelling supported driving as an optimal control cycle: Framework and model characteristics. *Transportation Research Part C Emerging Technologies*, 36:547–563, 06 2013. doi: 10.1016/j.trc.2013.06.012. URL <https://www.sciencedirect.com/science/article/pii/S1877042813009968?via%3Dihub>.
- [63] "asteroid mass distribution measurement with gravity gradiometers". [online] URL : <https://ui.adsabs.harvard.edu/abs/1971NASSP.267..585F/abstract> [Accessed : 03.20.2020].
- [64] Kieran Carroll. Measuring didymoon's mass using gravity gradiometry (maybe also surface gravimetry), 06 2017. URL https://www.researchgate.net/publication/318570602_Measuring_Didymoon%27s_Mass_Using_Gravity_Gradiometry_maybe_also_Surface_Gravimetry?channel=doi&linkId=5970c637aca272a59f76e8bc&showFulltext\unhbox\voidb@x\bgroup\let\unhbox\voidb@x\setbox\@tempboxa\hbox{t\global\mathchardef\accent@spacefactor\spacefactor}\accent22t\egroup\spacefactor\accent@spacefactorrue
- [65] "minor planet center" URL : <https://minorplanetcenter.net/data> [accessed : 01.16.2020].
- [66] "minor planet center" URL : http://sebago.mit.edu/near/NLR190_topo_model [accessed : 01.25.2020], .
- [67] Justin Atchison, Martin Ozimek, Brian Kantsiper, and Andrew Cheng. Trajectory options for the dart mission. *Acta Astronautica*, 123, 04 2016. doi: 10.1016/j.actaastro.2016.03.032. URL <https://www.sciencedirect.com/science/article/pii/S0094576515303040?via%3Dihub>.
- [68] Andris Slavinskis, Pekka Janhunen, P. Toivanen, Karri Muinonen, Antti Penttilä, Mikael Granvik, T. Kohout, Maria Gritsevich, Mihkel Pajusalu, Indrek Sünter, Hendrik Ehrpais, Janis Dalbins, Iaroslav Iakubivskyi, Tõnis Eenmäe, Erik Ilbis, David Mauro, Jan Stupl, Andrew Rivkin, and William Bottke. Nanospacecraft fleet for multi-asteroid touring with electric solar wind sails. *IEEE Aerospace Conference Proceedings*, 03 2018. doi: 10.1109/AERO.2018.8396670. URL <https://ieeexplore.ieee.org/document/8396670>.
- [69] "asteroid gravimetry" URL : <https://digitalcommons.usu.edu/cgi/viewcontent.cgi?article=3408context=smallsat> [accessed = 04.21.2020].
- [70] "keplerian orbital parameters". URL : <https://galileognss.eu/ephemeris-keplerian-parameters/> [Accessed : 28.07.2019].

9 Appendices

Study : False positive

A study was performed to test the algorithm’s performance in a scenario where the gravitational attraction for a particular zone within the body was way lower than the thrust exerted by the spacecraft. This zone was presumed to be a dust cloud or particle cloud. The spacecraft was made to orbit the SSSB in order test the motion planning performance.

Outcomes

It can be seen in figure 9.1 that the spacecraft escaped the SSSB’s sphere of influence as soon as it experienced lesser (almost negligible) force of attraction as compared to that of the thrust provided previously.

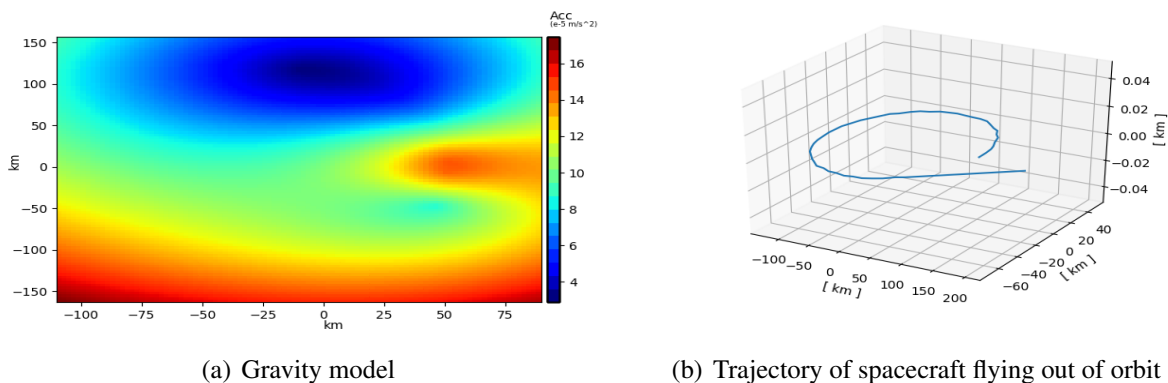


Figure 9.1: False positive study where the spacecraft flies out of orbit in absent gravity zone

Results Analysis

It can be analysed that the motion planner works with the consideration, that continuous gravitational attraction is acted upon it, that keeps it within the sphere of influence. A zone having almost negligible gravitational pull, shall tend to thrust away the spacecraft. The algorithm does not yet, account for maintaining the spacecraft trajectory in the absence of a gravitational force during explorations.

This is something that is worth considering for future work and development within the project.

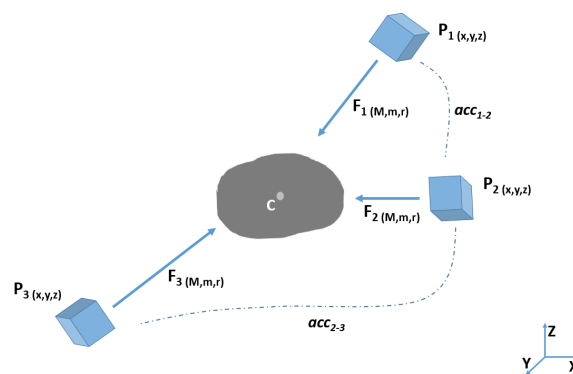
VEctor Gravimeter for Asteroids (VEGA)

The VECTOR Gravimeter for Asteroids [69] is a scientific instrument that can measure gravitational acceleration(s) with an isolated accelerometer within its housing. The gravimeter measures the gravity vectors without bias. Equipping the spacecraft with a VEGA instrument, the tidal gravitational forces exerted by the SSSB could be mapped in-orbit, by the changes in acceleration that are generated with the erratic changes in the gravitational force.

These perturbations can be mapped, to generate the acceleration field model around the body, at the particular distance at which it was measured.

Rationale	Value
Accuracy	1 - 10 nanoG on small asteroid
Size	9.5 x 9.5 x 18.5 cm
Power Consumption	4 - 12.5 W

Table 9.1: Specifics about VEGA Instrument



(a) VEGA Concept [64]



(b) VEGA Housing [69]

Figure 9.2: VECTOR Gravimeter for Asteroids

Keplerian Orbital Parameters

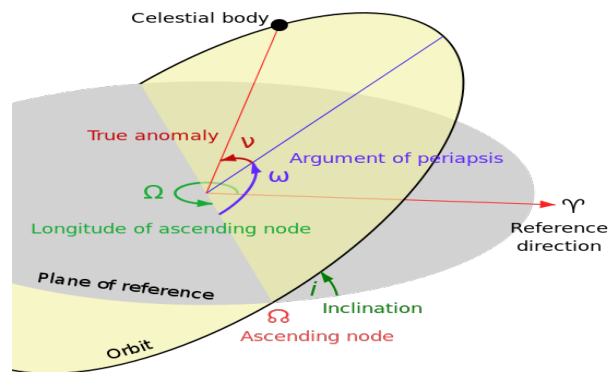


Figure 9.3: Graphical Representation of Keplerian Parameters
[70]

All bodies in the solar system revolve around the sun. Their orbits are defined by the Keplerian Laws which were laid by the German mathematician Johannes Kepler.

The orbital motion of the objects are explained by the 6 Keplerian elements [70] which define shape and size of the ellipse within which the bodies follow their trajectory. Figure 9.3 illustrated the Keplerian parameters that are briefly described below.

1. Eccentricity (e):
This defines the shape of the trajectory of the body (For a circular orbit $e = 0$; $e < 1$ for elliptical orbit; $e > 1$ for a hyperbolic trajectory and $e = 1$ for a parabolic trajectory).
2. Semi-major axis (a):
Defined by the the mean of sum of the periapsis (point of closest approach) and apoapsis (point of farthest motion) distances.
3. Inclination (i):
The vertical tilt of the ellipse with respect to the equatorial plane that is measures at the ascending node.
4. Longitude of the ascending node or right ascension of the ascending node (Ω):
The angle between the reference plane's vernal point and the ascending node.
5. Argument of periapsis (ω):
The angle measured from the ascending node to the periapsis. It defines the orientation of the ellipse in the orbital plane.
6. Mean anomaly (M):
Position of the spacecraft along the ellipse at a certain epoch.

Sphere of Gravitational Influence

Every body in the universe exerts an attractive force on other bodies towards its centre which is defined as the gravitational force of attraction. It is however noticeable that the force of attraction remains confined within a specific region around the body.

This region of gravitational influence for a particular body is termed as 'Sphere of Influence (SOI)' and is usually defined for larger bodies in space like planets and stars. In terms of conic approximation, the SOI is generally referred to as the boundary that causes a change in the trajectory of the orbiting body.

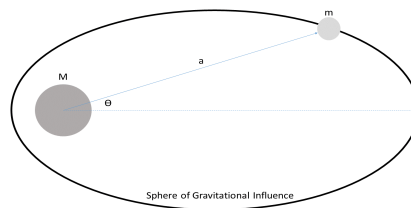


Figure 9.4: Sphere of Influence

Mathematically, the radius of the sphere of influence of a body m with a semi major orbit of a , orbiting around a large body of mass M is given by equation 9.1.

$$r_{SOI} \approx a \left(\frac{m}{M} \right)^{0.4} \quad (9.1)$$

For the Earth's r_{soi} wrt Sun,

$$\begin{aligned} \text{Mass of Earth } (m) &= 5.944e24 \text{ kg} \\ \text{Mass of Sun } (M) &= 1.989e30 \text{ kg} \\ \text{Semi Major Axis } (a) &= 1.49e8 \text{ km} \end{aligned}$$

$$r_{soi} \approx 1.49e8 \left(\frac{5.944e24}{1.989e30} \right)^{0.4}$$

$$r_{soi} \approx 0.924e6 \text{ km}$$

Software Information and Associated Libraries

Operating System(s)	Version	Description
Ubuntu	16.04 LTS	Operating System
Microsoft Windows	10 Home 1809	Operating System

Languages and Libraries	Version	Description
Python	3.7	Coding Environment
IDLE	Py3.7	Development Environment
HTML	5	Plotting
VPython	7.6.1	Visualizations
WebGL	1.0	Visualizations
AstroPy	4.0.1	Physics constants
Numpy	1.16	Library Support
Matplotlib	3.2.1	Plots
Mayavi	4.7.1	Plots
Scipy	1.4.1	Mathematics
Pandas	1.0.3	Data Read/Write/Analysis
VTK	8.1.2	Mayavi Support

Table 9.2: Software and Library information

Hardware Specifications

Hardware	Specifications
Processor	Intel(R) Core(TM) i5-8250U
Cores	4
System	64-bit x64
CPU frequency	1.60 GHz
RAM	6 Gb
Storage : HDD	1 Tb
Storage : SSD	256 Gb
Graphics Card	Intel UHD Graphics 620
BIOS	7SCN34WW

Table 9.3: Hardware Specifications

Non-exclusive licence to reproduce thesis and make thesis public

I, Aditya Savio Paul

1. herewith grant the University of Tartu a free permit (non-exclusive licence) to reproduce, for the purpose of preservation, including for adding to the DSpace digital archives until the expiry of the term of copyright,

“Autonomous motion planning for spacecrafts near small solar system bodies: simultaneously refining the gravitational field model and re-planning gravity dependant maneuvers”

supervised by Dr. Michael Otte and Mr. Viljo Allik

2. I grant the University of Tartu a permit to make the work specified in p. 1 available to the public via the web environment of the University of Tartu, including via the DSpace digital archives, under the Creative Commons licence CC BY NC ND 3.0, which allows, by giving appropriate credit to the author, to reproduce, distribute the work and communicate it to the public, and prohibits the creation of derivative works and any commercial use of the work until the expiry of the term of copyright.
3. I am aware of the fact that the author retains the rights specified in p. 1 and 2.
4. I certify that granting the non-exclusive licence does not infringe other persons' intellectual property rights or rights arising from the personal data protection legislation.

Aditya Savio Paul

20.05.2020